DISCONTINUOUS GALERKIN METHODS FOR 3D–1D SYSTEMS

RAMI MASRI*, MIROSLAV KUCHTA*, AND BEATRICE RIVIERE†

Abstract. We propose and analyze discontinuous Galerkin (dG) approximations to 3D-1D coupled systems which model diffusion in a 3D domain containing a small inclusion reduced to its 1D centerline. Convergence to weak solutions of a steady state problem is established via deriving a posteriori error estimates and bounds on residuals defined with suitable lift operators. For the time dependent problem, a backward Euler dG formulation is also presented and analysed. Further, we propose a dG method for networks embedded in 3D domains, which is, up to jump terms, locally mass conservative on bifurcation points. Numerical examples in idealized geometries portray our theoretical findings, and simulations in realistic 1D networks show the robustness of our method.

Key words. 3D-1D coupled models, discontinuous Galerkin methods, 1D vessel networks.

MSC codes. 65N30, 65M60.

1. Introduction. Modeling physiological processes involving the flow and transport within a complex network of vessel-like structures embedded in a 3D domain is crucial. Examples of such processes include drug transport in vascularized tissue [29, 3] and solute clearance through the lymphatic vessels in the body [27] and through the glymphatic system of the brain [26, 32]. This modeling setup has applications not only in physiology but also spans areas such as geosciences [13, 24].

To account for a complex network of vessels that typically have a small diameter compared to a surrounding domain, topological model reduction techniques have been proposed [6, 22]. Such models reduce the equations posed in 3D vessels to 1D equations posed on their centerlines. Further, these 1D equations are suitably coupled to extended 3D equations in the surrounding. Thereby, 3D–1D models reduce the computational cost while providing a reliable approximation to the full dimensional system. Bounds on the modeling error induced by such a derivation in terms of the vessel diameter are derived for the time dependent convection diffusion 3D-1D problem in [26], for the steady state diffusion 3D-1D problem in [22], and for the steady state 2D-0D problem in [19].

We remark that the 3D-1D model derived in [22] and further extended in [26] naturally uses the lateral average as a way to restrict 3D functions to 1D inclusions. This differs from the models presented in [4, 6], where 1D traces of 3D functions are used; therefore, the functional setting involves special weighted Hilbert spaces. The latter models can be generally viewed as elliptic problems with Dirac line sources. Several finite element schemes have been proposed and analyzed for this class of problems. In addition to the continuous Galerkin method introduced in [5] and further analyzed in [18, 8], we mention the singularity removal method [13], the mixed approach [14], the interior penalty dG method [25], and the Lagrange multiplier approach [21]. It is worth noting that the papers [13, 8, 14, 25] only analyze the 3D problem and assume a given 1D source term.

For the 3D-1D problem where the restriction operator is realized via lateral averages, the continuous Galerkin method is analyzed in [22], providing error estimates in energy norms. To the best of our knowledge, a discontinuous Galerkin method for the coupled 3D–1D system and its analysis are novel. DG approximations have several favorable features such as the local mass conservation property [28, Section 2.7.3]. In addition, with dG approximations, local mesh refinement and local high order approximation are easily handled since there are no continuity requirements. The analysis of dG for the coupled 3D–1D problem requires non–standard arguments as the strong consistency of the method cannot be assumed. This stems from the observation that the 3D so-

*Department of Numerical Analysis and Scientific Computing, Simula Research Laboratory, Oslo, 0164 Norway. (rami@simula.no, miroslav@simula.no).

†Department of Computational Applied Mathematics and Operations Research, Rice University, Houston, TX 77005, USA. (riviere@rice.edu).

Funding: RM gratefully acknowledges support from the Research Council of Norway (RCN) via FRIPRO grant agreement 324239 (EMIx). MK gratefully acknowledges support from the RCN grant 303326. BR is partially funded by NSF-DMS 2111459.

lution does not belong to $H^{3/2+\eta}(\Omega)$ for any positive η, the natural Sobolev space for the interior penalty dG bilinear form.

We now summarize the main contributions of the paper and give an outline of the contents.

- We propose an interior penalty dG method for the coupled 3D–1D problem, and we prove convergence to weak solutions. The main result is given in Theorem 4.6.
- We derive error estimates for regular meshes in Corollary 4.7 and for graded meshes in Corollary 4.8. The second estimate shows that if the mesh is resolved near the boundary of the inclusion, then almost optimal error rates are recovered.
- We analyze a backward Euler dG discretization for the time dependent problem by introducing a suitable interpolant which is based on the elliptic projection. The main result is in Theorem 5.1.
- For vessel networks embedded in a 3D domain, we propose a dG method with a hybridization technique on bifurcation points. Up to jump terms, this method preserves conservation of mass on such junctions, see Section 6. We show the well–posedness of this dG formulation.

The rest of this article is organized as follows. Sections 2 and 3 introduce the model problem and the dG approximation respectively. The error analysis for the steady state problem is included in Section 4. We analyze a backward Euler dG method for the transient 3D–1D model in Section 5. The case of a vessel network inside a 3D domain is studied in Section 6. In Section 7, we provide numerical examples for manufactured solutions in a 3D–1D setting, for 1D vessel networks, and for realistic 1D networks in 3D tissue. Conclusions follow in Section 8.

2. Model problem.

We introduce the needed notation and the steady state 3D-1D problem.

2.1. Notation.

Given an open domain $O \subset \mathbb{R}^d$, $d \in \{1,2,3\}$, the usual L^2 inner product is denoted by $(f,g)_O$ for given real functions f and g. Let $L^2(O)$ be the Hilbert space with inner product $(\cdot,\cdot)_O$ and the usual induced norm $\|\cdot\|_{L^2(O)}$. We drop the subscript when $O=\Omega$ and let $\|\cdot\| := \|\cdot\|_{L^2(\Omega)}$ and $(\cdot,\cdot) := (\cdot,\cdot)_\Omega$. Recall the notation of the standard Sobolev spaces $W^{m,p}(O)$ and $H^m(O) = W^{m,2}(O)$ for $m \in \mathbb{N}$ and $1 \le p \le \infty$. For a given weight $w \in L^\infty(O)$ and $w > 0$ a.e. in O, the weighted L^2 inner product is given by $(f,g)_{L^2_\omega(O)} = (f, wg)_O$ with the respective weighted L^2_ω space:

$$\|f\|_{L^2_w(O)} = \|w^{1/2} f\|_{L^2(O)},\ L^2_w(O) = \{f : O \to \mathbb{R} \mid \|f\|_{L^2_w(O)} < \infty\}. \tag{2.1}$$

Similarly, the weighted Hilbert space $H^1_w(O)$ is given by

$$H^1_w(O) = \{f \in L^2_w(O) \mid \|\nabla f\|_{L^2_w(O)} < \infty\}, \tag{2.2}$$

where the weighted inner product and norm are

$$(f,g)_{H^1_w(O)} = (f,g)_{L^2_w(O)} + (\nabla f, \nabla g)_{L^2_w(O)},\ \ \|f\|^2_{H^1_w(O)} = \|f\|^2_{L^2_w(O)} + \|\nabla f\|^2_{L^2_w(O)}. \tag{2.3}$$

We omit the subscript/weight w when $w = 1$. Throughout the paper, we denote by C a generic constant independent of mesh parameters. We use the standard notation $A \lesssim B$ for $A \le C\,B$ and $A \approx B$ for $A \le C\,B$ and $B \le C\,A$.

2.2. The 3D-1D model.

Let $\Omega \subset \mathbb{R}^3$ be a bounded domain with a one dimensional inclusion Λ. We assume that Λ is parametrized by $\boldsymbol{\lambda}(s), s \in [0,L]$ and is strictly included in Ω, $\boldsymbol{\lambda}$ is C^2 regular, and (for simplicity) $\|\boldsymbol{\lambda}'(s)\| = 1$ so that the arc length and s coincide. We further define B_Λ as a generalized cylinder with centerline Λ. The boundary of B_Λ will be denoted by Γ. See Figure 2.1 for an illustration of the considered geometry. A cross-section of B_Λ at $s \in [0,L]$ is denoted by $\Theta(s)$ with area $A(s)$ and perimeter $P(s)$. We assume that there are positive constants a_0, a_1 such that $a_0 \le A(s) + P(s) \le a_1$ for all s. We also assume that A belongs to $\mathcal{C}^1([0,L])$. For a function $u \in L^1(\partial\Theta(s))$, we define the lateral average $\bar{u}$ as

$$\overline{u}(s) = \frac{1}{P(s)} \int_{\partial\Theta(s)} u. \tag{2.4}$$

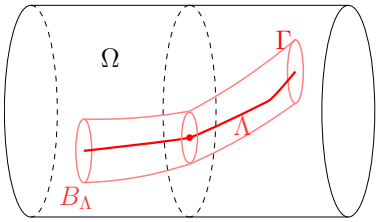

FIG. 2.1. *Illustration of the considered geometry*

The 3D-1D model that we consider results from a reduction of a 3D-3D model in $\Omega\backslash B_\Lambda$ and in B_Λ with Robin type interface conditions on Γ. This condition models the membrane Γ as semi-permeable with permeability constant $\xi > 0$. Averaging the equations in B_Λ and formally extending the equations in $\Omega\backslash B_\Lambda$, one obtains the following coupled system.

$$-\Delta u + \xi(\overline{u} - \hat{u})\delta_\Gamma = f \quad \text{in } \Omega, \tag{2.5}$$

$$-\mathrm{d}_s(A\,\mathrm{d}_s\hat{u}) + P\,\xi(\hat{u} - \overline{u}) = A\,\hat{f} \ \text{ in } \Lambda. \tag{2.6}$$

The source terms $f \in L^2(\Omega)$ and $\hat{f} \in L^2_A(\Lambda)$ are given. We refer to [22, 26] for details on the derivation and on the model error analysis. The above equations are to be understood in the weak sense, and the functional $(\overline{u} - \hat{u})\delta_\Gamma$ is defined over $H^1(\Omega)$ as

$$(\overline{u} - \hat{u})\delta_\Gamma(v) = \int_\Lambda P(\overline{u} - \hat{u})\overline{v}, \quad \forall v \in H^1(\Omega). \tag{2.7}$$

The above functional is well-defined since an application of Cauchy-Schwarz's inequality and trace theorem yields

$$\|\overline{v}\|_{L^2_P(\Lambda)} \leq \|v\|_{L^2(\Gamma)} \lesssim \|v\|_{H^1(\Omega)}, \quad \forall v \in H^1(\Omega). \tag{2.8}$$

The system (2.5)–(2.6) is complemented by the following boundary conditions.

$$u = 0 \ \text{ on } \partial\Omega, \quad \text{and} \quad A\,\mathrm{d}_s\hat{u} = 0 \ \text{ on } s = \{0, L\}. \tag{2.9}$$

To introduce the weak formulation of (2.5)–(2.6), we define the following bilinear forms.

$$a(u, v) = (\nabla u, \nabla v), \qquad \forall u, v \in H^1(\Omega), \tag{2.10}$$

$$a_\Lambda(\hat{u}, \hat{v}) = (\mathrm{d}_s\hat{u}, \mathrm{d}_s\hat{v})_{L^2_A(\Lambda)}, \quad \forall \hat{u}, \hat{v} \in H^1_A(\Lambda), \tag{2.11}$$

$$b_\Lambda(\hat{v}, \hat{w}) = (\xi\hat{v}, \hat{w})_{L^2_P(\Lambda)}, \qquad \forall \hat{v}, \hat{w} \in L^2_P(\Lambda). \tag{2.12}$$

The weak formulation of the coupled 3D-1D problem then reads [22]: Find $\boldsymbol{u} = (u, \hat{u}) \in H^1_0(\Omega) \times H^1_A(\Lambda)$ such that

$$a(u, v) + b_\Lambda(\overline{u} - \hat{u}, \overline{v}) = (f, v)_\Omega, \qquad \forall v \in H^1_0(\Omega), \tag{2.13}$$

$$a_\Lambda(\hat{u}, \hat{v}) + b_\Lambda(\hat{u} - \overline{u}, \hat{v}) = (\hat{f}, \hat{v})_{L^2_A(\Lambda)}, \quad \forall \hat{v} \in H^1_A(\Lambda). \tag{2.14}$$

The terms given in b_Λ model the coupling between the 3D solution u and the 1D solution $\hat{u}$. Equivalently, one can write the above as follows. Find $\boldsymbol{u} = (u, \hat{u}) \in H^1_0(\Omega) \times H^1_A(\Lambda)$ such that

$$\mathcal{A}(\boldsymbol{u}, \boldsymbol{v}) = (f, v)_\Omega + (\hat{f}, \hat{v})_{L^2_A(\Lambda)}, \quad \forall \boldsymbol{v} = (v, \hat{v}) \in H^1_0(\Omega) \times H^1_A(\Lambda), \tag{2.15}$$

where we define for $\boldsymbol{u} = (u, \hat{u}), \boldsymbol{v} = (v, \hat{v}) \in H^1_0(\Omega) \times H^1_A(\Lambda)$

$$\mathcal{A}(\boldsymbol{u}, \boldsymbol{v}) = a(u, v) + a_\Lambda(\hat{u}, \hat{v}) + b_\Lambda(\overline{u} - \hat{u}, \overline{v} - \hat{v}). \tag{2.16}$$

The problem given in (2.15) is well-posed, see [22, Section 3.2].

3. Discontinuous Galerkin formulation. The numerical method is presented here.

3.1. Meshes and dG spaces. We consider a family of regular partitions of Ω made of tetrahedra and denoted by $\mathcal{T}_\Omega^h$. The mesh-size is $h = \max_{K\in\mathcal{T}_\Omega^h} h_K$, where $h_K = \text{diam}(K)$. We associate with $\mathcal{T}_\Omega^h$, the space $H^1(\mathcal{T}_\Omega^h)$ of broken H^1 functions in Ω, and a finite dimensional space $\mathbb{V}_h^\Omega$ of broken piecewise polynomials of order k_1.

$$\mathbb{V}_h^\Omega = \{v_h \in L^2(\Omega),\ \ v_h \in \mathbb{P}_{k_1}(K),\ \ \forall K \in \mathcal{T}_\Omega^h\}. \tag{3.1}$$

We let $\mathcal{T}_\Lambda^h = \{(s_{i-1}, s_i),\ i = 1, \ldots, N\}$ with $s_0 = 0$ and $s_N = L$ be a family of uniform partitions of $[0, L]$, with mesh size $h_\Lambda = s_i - s_{i-1}$. This mesh over $[0, L]$ defines a partition of the curve Λ via the parameterization $\boldsymbol{\lambda}$: each element (s_{i-1}, s_i) defines a curved part of Λ via the mapping $\boldsymbol{\lambda}$. Note that we will not refer to or use these curved elements as the reference domain is $(0, L)$. We let $H^1(\mathcal{T}_\Lambda^h)$ be the space of broken H^1 functions in $(0, L)$, and we let $\mathbb{V}_h^\Lambda$ be the respective space of broken piecewise polynomials of order k_2.

$$\mathbb{V}_h^\Lambda = \{\hat{v}_h \in L^2((0, L)),\ \ \hat{v}_h \in \mathbb{P}_{k_2}((s_{i-1}, s_i)),\ \ 1 \le i \le N\}. \tag{3.2}$$

Note that with the parameterization, functions in $H^1(\mathcal{T}_\Lambda^h)$ and in $\mathbb{V}_h^\Lambda$ define functions in the broken $H^1(\Lambda)$ space by setting $v := \hat{v} \circ \boldsymbol{\lambda}^{-1}$. While this observation highlights that we are essentially using a Galerkin subspace of the broken $H^1(\Lambda)$ space, it will not be used or referred to in the analysis that follows.

For each $1 \le i \le N$, we let B_i be the portion of B_Λ obtained when s is restricted to $\Lambda_i = (s_{i-1}, s_i)$. That is, we have that

$$\bigcup_{1\le i\le N} B_i = B_\Lambda.$$

For each $1 \le i \le N$, we now define neighborhoods of the curve between $\boldsymbol{\lambda}(s_{i-1})$ and $\boldsymbol{\lambda}(s_i)$ consisting of 3D elements in $\mathcal{T}_\Omega^h$. Namely, we define

$$\omega_i = \{K \in \mathcal{T}_\Omega^h,\ \ K \cap \partial B_i \neq \emptyset\}. \tag{3.3}$$

We can then write

$$\mathcal{T}_B^h := \{K \in \mathcal{T}_\Omega^h,\ \ K \cap \partial B_\Lambda \neq \emptyset\} = \bigcup_{1\le i\le N} \omega_i. \tag{3.4}$$

We assume that if $K \cap B_\Lambda \neq \emptyset$, then the two-dimensional Lebesgue measure of $\partial K \cap \partial B_\Lambda$ is zero. This ensures that the term $b_\Lambda(\cdot, \cdot)$ involving the average operator given in (2.4) is well defined for $H^1(\mathcal{T}_\Omega^h)$.

Further, we assume the following relation between the level of refinement for the 3D domain and that of the 1D domain. For $K \in \mathcal{T}_B^h$, let $\mathcal{I}_K$ be the set of integers i_0 such that $K \in \omega_{i_0}$. We assume that the cardinality of $\mathcal{I}_K$ is bounded above by a constant independent of K and of h. Essentially, this assumption means the 3D mesh intersecting ∂B_Λ can not remain fixed while the 1D mesh is refined.

We also denote by Γ_h the set of all interior faces in $\mathcal{T}_\Omega^h$. The set of edges belonging to elements in $\mathcal{T}_B^h$ is decomposed by defining

$$\Gamma_i = \{F \in \Gamma_h,\ \ F \subset \partial K,\ \text{ where } \ K \in \omega_i\}. \tag{3.5}$$

For each interior face F, we associate a unit normal vector $\boldsymbol{n}_F$ and we denote by K_F^1 and K_F^2 the two elements that share F such that the vector $\boldsymbol{n}_F$ points from K_F^1 to K_F^2. We denote the average and the jump of a function $v_h \in \mathbb{V}_h^\Omega$ by $\{v_h\}$ and $[v_h]$ respectively.

$$\{v_h\}|_F = \frac{1}{2}\left(v_h|_{K_F^1} + v_h|_{K_F^2}\right), \quad [v_h]|_F = v_h|_{K_F^1} - v_h|_{K_F^2}, \quad \forall F \in \Gamma_h. \tag{3.6}$$

If $F = \partial\Omega \cap \partial K_F^1$, then the average and the jump are given by

$$[v]|_F = \{v\}|_F = v|_{K_F^1}. \tag{3.7}$$

The area of $F \in \Gamma_h \cup \partial\Omega$ is denoted by $|F|$. Similar definitions are adopted for jumps and averages of $\hat{v}_h \in \mathbb{V}_h^\Lambda$ on the nodes s_i.

$$\begin{aligned} 1 \le i \le N-1, \quad [\hat{v}_h]_{s_i} &= \lim_{t\to 0, t>0} \hat{v}_h(s_i - t) - \lim_{t\to 0, t>0} \hat{v}_h(s_i + t), \\ 1 \le i \le N-1, \quad \{\hat{v}_h\}_{s_i} &= \frac{1}{2} \lim_{t\to 0, t>0} \hat{v}_h(s_i + t) + \frac{1}{2} \lim_{t\to 0, t>0} \hat{v}_h(s_i - t), \\ [\hat{v}_h]_{s_0} &= -\hat{v}_h(s_0), \quad [\hat{v}_h]_{s_N} = \hat{v}_h(s_N). \end{aligned}$$

For $v \in H^1(\mathcal{T}_\Omega^h)$, we define the norm for $\sigma_\Omega > 0$

$$\|v\|_{\mathbb{V}_h^\Omega}^2 = \sum_{K\in\mathcal{T}_\Omega^h} \|\nabla v\|_{L^2(K)}^2 + \sum_{F\in\Gamma_h\cup\partial\Omega} \frac{\sigma_\Omega}{|F|^{1/2}} \|[v]\|_{L^2(F)}^2. \tag{3.8}$$

A Poincaré inequality holds in $H^1(\mathcal{T}_\Omega^h)$ (see for e.g [7, Remark 4.15]):

$$\|v\|_{L^2(\Omega)} \lesssim \|v\|_{\mathbb{V}_h^\Omega}, \quad \forall v \in H^1(\mathcal{T}_\Omega^h). \tag{3.9}$$

For $\hat{v} \in H^1(\mathcal{T}_\Lambda^h)$, we define the semi-norm for $\sigma_\Lambda > 0$

$$|\hat{v}|_{\mathbb{V}_h^\Lambda}^2 = \sum_{i=1}^N \|\mathrm{d}_s \hat{v}\|_{L^2((s_{i-1},s_i))}^2 + \sum_{i=1}^{N-1} \frac{\sigma_\Lambda}{h_\Lambda} [\hat{v}]_{s_i}^2. \tag{3.10}$$

The above definitions allow us to introduce the norm $\|\cdot\|_{\mathrm{DG}}$ on $H^1(\mathcal{T}_\Omega^h) \times H^1(\mathcal{T}_\Lambda^h)$. For $\boldsymbol{v} = (v, \hat{v})$,

$$\|\boldsymbol{v}\|_{\mathrm{DG}}^2 = \|v\|_{\mathbb{V}_h^\Omega}^2 + |\hat{v}|_{\mathbb{V}_h^\Lambda}^2 + \|\overline{v} - \hat{v}\|_{L_P^2(\Lambda)}^2. \tag{3.11}$$

The above indeed defines a norm. If $\|\boldsymbol{v}\|_{\mathrm{DG}} = 0$, then $v = 0$ since $\|\cdot\|_{\mathbb{V}_h^\Omega}$ is a norm on $H^1(\mathcal{T}_\Omega^h)$. This implies that $\|\hat{v}\|_{L_P^2(\Lambda)} = 0$ and $\hat{v} = 0$.

3.2. The numerical method. We use interior penalty discontinuous Galerkin forms [28]. Define $a_h(\cdot,\cdot) : \mathbb{V}_h^\Omega \times \mathbb{V}_h^\Omega \to \mathbb{R}$:

$$\begin{aligned} a_h(u,v) = &\sum_{K\in\mathcal{T}_\Omega^h} \int_K \nabla u \cdot \nabla v - \sum_{F\in\Gamma_h\cup\partial\Omega} \int_F \{\nabla u\} \cdot \boldsymbol{n}_F [v] \\ &+\epsilon_1 \sum_{F\in\Gamma_h\cup\partial\Omega} \int_F \{\nabla v\} \cdot \boldsymbol{n}_F [u] + \sum_{F\in\Gamma_h\cup\partial\Omega} \frac{\sigma_\Omega}{|F|^{1/2}} \int_F [u][v]. \end{aligned} \tag{3.12}$$

For the 1D discrete solution, we introduce the form $a_{\Lambda,h}(\cdot,\cdot) : \mathbb{V}_h^\Lambda \times \mathbb{V}_h^\Lambda \to \mathbb{R}$

$$\begin{aligned} a_{\Lambda,h}(\hat{u},\hat{v}) = &\sum_{i=1}^N \int_{s_{i-1}}^{s_i} A \frac{\mathrm{d}\hat{u}}{\mathrm{d}s} \frac{\mathrm{d}\hat{v}}{\mathrm{d}s} - \sum_{i=1}^{N-1} \left\{ A \frac{\mathrm{d}\hat{u}}{\mathrm{d}s} \right\}_{s_i} [\hat{v}]_{s_i} \\ &+ \epsilon_2 \sum_{i=1}^{N-1} \left\{ A \frac{\mathrm{d}\hat{v}}{\mathrm{d}s} \right\}_{s_i} [\hat{u}]_{s_i} + \sum_{i=1}^{N-1} \frac{\sigma_\Lambda}{h_\Lambda} [\hat{u}]_{s_i} [\hat{v}]_{s_i}. \end{aligned} \tag{3.13}$$

In the above, $\epsilon_1, \epsilon_2 \in \{-1, 0, 1\}$ lead to symmetric, incomplete, or non-symmetric discretizations, and $\sigma_\Lambda, \sigma_\Omega > 0$ are penalty parameters. The dG formulation of problem (2.15) then reads as follows. Find $\boldsymbol{u}_h = (u_h, \hat{u}_h) \in \mathbb{V}_h^\Omega \times \mathbb{V}_h^\Lambda$ such that

$$\mathcal{A}_h(\boldsymbol{u}_h, \boldsymbol{v}_h) = (f, v_h)_\Omega + (\hat{f}, \hat{v}_h)_\Lambda, \quad \forall \boldsymbol{v}_h = (v_h, \hat{v}_h) \in \mathbb{V}_h^\Omega \times \mathbb{V}_h^\Lambda, \tag{3.14}$$

where we defined the form $\mathcal{A}_h(\cdot,\cdot) : (\mathbb{V}_h^\Omega \times \mathbb{V}_h^\Lambda)^2 \to \mathbb{R}$:

$$\mathcal{A}_h(\boldsymbol{u}_h, \boldsymbol{v}_h) = a_h(u_h, v_h) + a_{\Lambda,h}(\hat{u}_h, \hat{v}_h) + b_\Lambda(\overline{u}_h - \hat{u}_h, \overline{v}_h - \hat{v}_h). \tag{3.15}$$

It is important to note that the interface Γ does not need to be resolved by the mesh to realize the coupling term b_Λ; identifying the elements intersecting Γ is sufficient. To show the well–posedness of the discrete dG formulation, we first show the coercivity of $\mathcal{A}_h$ with respect to the norm defined in (3.11).

LEMMA 3.1 (Coercivity). *For suitably chosen penalty parameters σ_Λ and σ_Ω, there exists a constant C_{coerc} such that*

$$\mathcal{A}_h(\boldsymbol{u}_h, \boldsymbol{u}_h) \geq C_{\text{coerc}} \|\boldsymbol{u}_h\|_{\text{DG}}^2, \quad \forall \boldsymbol{u}_h \in \mathbb{V}_h^\Omega \times \mathbb{V}_h^\Lambda. \tag{3.16}$$

Proof. If σ_Ω is large enough whenever $\epsilon_1 = -1$ or for any σ_Ω when $\epsilon_1 = 1$ (same conditions apply for σ_Λ and ϵ_2), we have that

$$a_h(u_h, u_h) \geq C_1 \|u_h\|_{\mathbb{V}_h^\Omega}^2, \quad a_{\Lambda,h}(\hat{u}_h, \hat{u}_h) \geq C_2 |\hat{u}_h|_{\mathbb{V}_h^\Lambda}^2. \tag{3.17}$$

Note that the proofs of the above estimates are immediate for the case $\epsilon_1 = \epsilon_2 = 1$. For the other cases, careful applications of discrete trace estimates and Cauchy–Schwarz's inequality yield the results. The details of the proofs follow standard arguments, see for e.g. [28, Section 2.7.1]. The result then immediately follows from the above and from the definition of $\mathcal{A}_h(\cdot,\cdot)$. ∎

LEMMA 3.2 (Existence and uniqueness of solutions). *There exists a unique pair $(u_h, \hat{u}_h) \in \mathbb{V}_h^\Omega \times \mathbb{V}_h^\Lambda$ solving (3.14).*

Proof. From the coercivity property, it easily follows that the solution is unique. Since this is a square linear system in finite dimensions, existence follows. ∎

4. Error analysis. The main difficulty in the error analysis of the dG formulation is that the strong consistency of the method can not be assumed. Indeed, under sufficient regularity assumptions on the domain, one can only show that the 3D solution u of (2.15) belongs to $H^{3/2-\eta}(\Omega)$ for $\eta > 0$ [22]. However, the form a_h can not be extended to this space since the traces of gradients for functions in $H^{3/2-\eta}(\Omega)$ are not well–defined. Therefore, we adopt here a combination of a priori and a posteriori error estimates within the framework proposed by Gudi [16] to prove convergence. The main result is provided in Theorem 4.6.

4.1. Preliminary lemmas. We first introduce the conforming spaces $\mathbb{V}_{h,c}^\Omega \subset H_0^1(\Omega)$ of continuous piecewise linear functions defined over $\mathcal{T}_\Omega^h$ in Ω. Similarly, we let $\mathbb{V}_{h,c}^\Lambda$ be the respective space of continuous piecewise linear functions defined over $\mathcal{T}_\Lambda^h$.

LEMMA 4.1. *There exists an enriching map $\boldsymbol{E} = (E, \hat{E}) : \mathbb{V}_h^\Omega \times \mathbb{V}_h^\Lambda \to \mathbb{V}_{h,c}^\Omega \times \mathbb{V}_{h,c}^\Lambda$ such that*

$$|Ev|_{H^1(\Omega)} \lesssim \|v\|_{\mathbb{V}_h^\Omega}, \quad |\hat{E}\hat{v}|_{H^1(\Lambda)} \lesssim |\hat{v}|_{\mathbb{V}_h^\Lambda}, \tag{4.1}$$

$$\left(\sum_{K \in \mathcal{T}_\Omega^h} h_K^{-2} \|Ev - v\|_{L^2(K)}^2 \right)^{1/2} \lesssim \|v\|_{\mathbb{V}_h^\Omega}, \quad \|\hat{E}\hat{v} - \hat{v}\|_{L^2(\Lambda)} \lesssim h_\Lambda |\hat{v}|_{\mathbb{V}_h^\Lambda}. \tag{4.2}$$

Proof. An enriching map with the above properties can be constructed as a nodal Lagrange interpolant with nodal values taken as averages of v ($\hat{v}$), see [17, Theorem 2.2] and [7, Section 5.5.2]. Another approach is to apply a Scott-Zhang interpolant to a Crouzeix-Raviart correction, see [12, Lemma 6.2]. ∎

We now define L^2–projections. Let $K \in \mathcal{T}_\Omega^h$ and $\Lambda_i = (s_{i-1}, s_i)$ for $i \in \{1, \ldots, N\}$. For any $(w, \hat{w}) \in L^2(K) \times L^2(\Lambda_i)$, define $(\pi_h w, \hat{\pi}_h \hat{w}) \in \mathbb{P}^{k_1}(K) \times \mathbb{P}^{k_2}(\Lambda_i)$ such that

$$\forall v_h \in \mathbb{P}^{k_1}(K), \quad (\pi_h w - w, v_h)_K = 0, \quad \forall \hat{v}_h \in \mathbb{P}^{k_2}(\Lambda_i), \quad (\hat{\pi}_h \hat{w} - \hat{w}, \hat{v}_h)_{L_P^2(\Lambda_i)} = 0. \tag{4.3}$$

LEMMA 4.2 (Properties of the L^2–projections). *Let $s \in \{0,\dots,k+1\}$, $m \in \{0,\dots,s\}$, $K \in \mathcal{T}_\Omega^h$, and $\Lambda_i = (s_{i-1}, s_i)$ for $i \in \{1,\dots,N\}$. Assume that $w \in H^s(K)$ and $\hat{w} \in H^s(\Lambda_i)$. Then,*

$$\|\pi_h w - w\|_{H^m(K)} \lesssim h_K^{s-m} \|w\|_{H^s(K)}, \quad \|\hat{\pi}_h \hat{w} - \hat{w}\|_{H^m(\Lambda_i)} \lesssim h_\Lambda^{s-m} \|\hat{w}\|_{H^s(\Lambda_i)}. \tag{4.4}$$

In addition, the L^2 projection is stable in the dG norm. Namely,

$$\|\pi_h w\|_{\mathbb{V}_h^\Omega} \lesssim \|w\|_{H^1(\mathcal{T}_\Omega^h)}, \quad \forall w \in H^1(\mathcal{T}_\Omega^h). \tag{4.5}$$

Proof. Proofs of the estimates in (4.4) can be found in [7, Lemma 1.58]. The proof of (4.5) follows from applications of trace estimates and (4.4). ∎

We now state a local trace inequality on ∂B_Λ. The proof of the following estimate is due to Wu and Xiao [33, Lemma 3.1].

LEMMA 4.3 (Local trace estimate on ∂B_Λ). *There exists a constant h_0 such that for all $h \le h_0$ and $K \in \mathcal{T}_B^h$, the following estimates hold*

$$\|v\|_{L^2(\partial B_\Lambda \cap \overline{K})} \lesssim h_K^{-1/2} \|v\|_{L^2(K)} + h_K^{1/2} \|\nabla v\|_{L^2(K)}, \quad \forall v \in H^1(K), \tag{4.6}$$

$$\|v_h\|_{L^2(\partial B_\Lambda \cap \overline{K})} \lesssim h_K^{-1/2} \|v_h\|_{L^2(K)}, \qquad \forall v_h \in \mathbb{P}_k(K), \quad \forall k \ge 1. \tag{4.7}$$

Hereinafter, we assume that $h \le h_0$. We now show a global trace inequality.

LEMMA 4.4 (Trace estimate). *For $u \in H^1(\mathcal{T}_\Omega^h)$, there holds*

$$\|\overline{u}\|_{L^2_P(\Lambda)} \lesssim \|u\|_{\mathbb{V}_h^\Omega}. \tag{4.8}$$

Proof. We start by showing the result for $v_h \in \mathbb{V}_h^\Omega$. Let $\Lambda_i = (s_{i-1}, s_i)$. We use triangle and Cauchy–Schwarz's inequalities to obtain that for any $1 \le i \le N$,

$$\|\overline{v_h}\|_{L^2_P(\Lambda_i)} \le \|\overline{v_h} - \overline{Ev_h}\|_{L^2_P(\Lambda_i)} + \|\overline{Ev_h}\|_{L^2_P(\Lambda_i)} \le \|v_h - Ev_h\|_{L^2(\partial B_i)} + \|\overline{Ev_h}\|_{L^2_P(\Lambda_i)}. \tag{4.9}$$

Recall the definition of ω_i in (3.3) and note that

$$\|v_h - Ev_h\|^2_{L^2(\partial B_i)} = \sum_{K \in \omega_i} \|v_h - Ev_h\|^2_{L^2(\partial B_i \cap \bar{K})}. \tag{4.10}$$

With (4.7), we obtain that

$$\|v_h - Ev_h\|^2_{L^2(\partial B_i)} \lesssim \sum_{K \in \omega_i} h_K^{-1} \|v_h - Ev_h\|^2_{L^2(K)}.$$

Summing over i and using the global bound (4.2) yield

$$\sum_{i=1}^N \|v_h - Ev_h\|^2_{L^2(\partial B_i)} \lesssim \sum_{K \in \mathcal{T}_B^h} h_K^{-1} \|v_h - Ev_h\|^2_{L^2(K)} \lesssim h \|v_h\|^2_{\mathbb{V}_h^\Omega}.$$

Therefore, with (2.8), we obtain

$$\|\overline{v_h}\|^2_{L^2_P(\Lambda)} = \sum_{i=1}^N \|\overline{v_h}\|^2_{L^2_P(\Lambda_i)} \lesssim h \|v_h\|^2_{\mathbb{V}_h^\Omega} + \|\overline{Ev_h}\|^2_{L^2_P(\Lambda)} \lesssim h \|v_h\|^2_{\mathbb{V}_h^\Omega} + \|Ev_h\|^2_{H^1(\Omega)}. \tag{4.11}$$

With Poincaré's inequality (3.9), and the properties of E (4.1)–(4.2), we obtain the bound

$$\|Ev_h\|^2_{H^1(\Omega)} \le \|Ev_h - v_h\|^2_{L^2(\Omega)} + \|v_h\|^2_{L^2(\Omega)} + |Ev_h|^2_{H^1(\Omega)} \lesssim \|v_h\|^2_{\mathbb{V}_h^\Omega}.$$

Substituting the above in (4.11) yields (4.8) for $v_h \in \mathbb{V}_h^\Omega$. Consider now $u \in H^1(\mathcal{T}_\Omega^h)$ and recall that $\pi_h u$ is the local L^2 projection on $\mathbb{V}_h^\Omega$. Then, by Cauchy–Schwarz's inequality and (4.6), we have that

$$\begin{aligned}\|\overline{u} - \overline{\pi_h u}\|^2_{L^2_P(\Lambda_i)} &\leq \sum_{K\in\omega_i} \|u - \pi_h u\|^2_{L^2(\partial B_i \cap \overline{K})} \\ &\lesssim \sum_{K\in\omega_i} \left(h_K^{-1}\|u-\pi_h u\|^2_{L^2(K)} + h_K \|\nabla(u-\pi_h u)\|^2_{L^2(K)}\right) \lesssim \sum_{K\in\omega_i} h_K \|u\|^2_{H^1(K)}.\end{aligned}$$

In the above, we used the properties of the L^2 projection given in (4.4). Then, using triangle inequality and (4.8) for $\mathbb{V}_h^\Omega$, we obtain

$$\|\overline{u}\|_{L^2_P(\Lambda)} \leq \|\overline{u} - \overline{\pi_h u}\|_{L^2_P(\Lambda)} + \|\overline{\pi_h u}\|_{L^2_P(\Lambda)} \lesssim h^{1/2} (\sum_{K\in\mathcal{T}_\Omega^h} \|u\|^2_{H^1(K)})^{1/2} + \|\pi_h u\|_{\mathbb{V}_h^\Omega}. \tag{4.12}$$

The result is concluded by Poincaré's inequality (3.9) and the stability of the L^2 projection π_h in the $\|\cdot\|_{\mathbb{V}_h^\Omega}$ norm, see (4.5). ∎

A consequence of (4.8) and the triangle inequality is the following bound:

$$\forall \boldsymbol{u} = (u, \hat{u}) \in H^1(\mathcal{T}_\Omega^h) \times H^1(\mathcal{T}_\Lambda^h), \quad \|\hat{u}\|_{L^2_P(\Lambda)} \lesssim \|\boldsymbol{u}\|_{\mathrm{DG}}. \tag{4.13}$$

We will make use of lift operators. For a given $(u, \hat{u}) \in H^1(\mathcal{T}_\Omega^h) \times H^1(\mathcal{T}_\Lambda^h)$, define $(L_h u, \hat{L}_h \hat{u}) \in \mathbb{V}_h^\Omega \times \mathbb{V}_h^\Lambda$ such that

$$(L_h u, w_h)_\Omega + (\hat{L}_h \hat{u}, \hat{w}_h)_{L^2_P(\Lambda)} = b_\Lambda(\overline{u} - \hat{u}, \overline{w}_h - \hat{w}_h), \quad \forall (w_h, \hat{w}_h) \in \mathbb{V}_h^\Omega \times \mathbb{V}_h^\Lambda. \tag{4.14}$$

The existence of $(L_h u, \hat{L}_h \hat{u})$ easily follows from uniqueness. We show the following estimate.

Lemma 4.5 (Lift operator). *Given $(u, \hat{u}) \in H^1(\mathcal{T}_\Omega^h) \times H^1(\mathcal{T}_\Lambda^h)$, let $(L_h u, \hat{L}_h \hat{u}) \in \mathbb{V}_h^\Omega \times \mathbb{V}_h^\Lambda$ be defined by (4.14). There holds*

$$\sum_{K\in\mathcal{T}_\Omega^h} h_K \|L_h u\|^2_{L^2(K)} + \|\hat{L}_h \hat{u}\|^2_{L^2_P(\Lambda)} \lesssim \|u\|^2_{\mathbb{V}_h^\Omega} + \|\hat{u}\|^2_{L^2_P(\Lambda)}. \tag{4.15}$$

Proof. Choosing $(w_h, \hat{w}_h) = (0, \hat{L}_h \hat{u})$ in (4.14) and using Cauchy-Schwarz's inequality and (4.8), we have

$$\|\hat{L}_h \hat{u}\|^2_{L^2_P(\Lambda)} \leq \xi \|\overline{u} - \hat{u}\|_{L^2_P(\Lambda)} \|\hat{L}_h \hat{u}\|_{L^2_P(\Lambda)} \lesssim (\|u\|_{\mathbb{V}_h^\Omega} + \|\hat{u}\|_{L^2_P(\Lambda)}) \|\hat{L}_h \hat{u}\|_{L^2_P(\Lambda)}. \tag{4.16}$$

This shows the bound on the second term in (4.15). Next, fix $K \in \mathcal{T}_B^h$ and recall that $\mathcal{I}_K$ be the set of integers i_0 such that $K \in \omega_{i_0}$ where we assume that the cardinality of $\mathcal{I}_K$ is bounded above by a small constant independent of K. In (4.14), choose $\hat{w}_h = 0$ and $w_h = (L_h u)\chi_K$ where χ_K is the characteristic function on K. We obtain

$$\|L_h u\|^2_{L^2(K)} \lesssim \sum_{i_0 \in \mathcal{I}_K} (\|\overline{u}\|_{L^2_P((s_{i_0-1}, s_{i_0}))} + \|\hat{u}\|_{L^2_P((s_{i_0-1}, s_{i_0}))}) \|\overline{w}_h\|_{L^2_P((s_{i_0-1}, s_{i_0}))}. \tag{4.17}$$

We now use Cauchy–Schwarz's inequality, the observation that w_h is locally supported in K, and trace inequality (4.7). We estimate

$$\|\overline{w}_h\|_{L^2_P((s_{i_0-1}, s_{i_0}))} \leq \|w_h\|_{L^2(\partial B_{i_0})} = \|L_h u\|_{L^2(\partial B_{i_0} \cap \bar{K})} \lesssim h_K^{-1/2} \|L_h u\|_{L^2(K)}. \tag{4.18}$$

Thus, we conclude that

$$\|L_h u\|^2_{L^2(K)} \lesssim h_K^{-1/2} \sum_{i_0 \in \mathcal{I}_K} (\|\overline{u}\|_{L^2_P((s_{i_0-1}, s_{i_0}))} + \|\hat{u}\|_{L^2_P((s_{i_0-1}, s_{i_0}))}) \|L_h u\|_{L^2(K)}. \tag{4.19}$$

Summing the above bound over $K \in \mathcal{T}_B^h$ and using Cauchy-Schwarz's inequality yield

$$\sum_{K\in\mathcal{T}_B^h} h_K \|L_h u\|^2_{L^2(K)} \lesssim (\|\overline{u}\|_{L^2_P(\Lambda)} + \|\hat{u}\|_{L^2_P(\Lambda)}) \left(\sum_{K\in\mathcal{T}_B^h} h_K \|L_h u\|^2_{L^2(K)} \right)^{1/2}.$$

With Lemma 4.4 and with noting that $L_h u|_K = 0$ for $K \notin \mathcal{T}_B^h$, we conclude the result. ∎

4.2. Main result and proof outline. The main convergence result reads as follows.

THEOREM 4.6. *Let $\boldsymbol{u} = (u, \hat{u}) \in H^1_0(\Omega) \times H^1(\Lambda)$ be the weak solution defined by (2.15), and let $\boldsymbol{u}_h = (u_h, \hat{u}_h) \in \mathbb{V}_h^\Omega \times \mathbb{V}_h^\Lambda$ be the discrete solution defined by (3.14). Recall that $h_B = \max_{K\in\mathcal{T}_B^h} h_K$. The following estimate holds.*

$$\|\boldsymbol{u} - \boldsymbol{u}_h\|_{\mathrm{DG}} \lesssim \inf_{\boldsymbol{v}\in\mathbb{V}_h^\Omega\times\mathbb{V}_h^\Lambda} \|\boldsymbol{u} - \boldsymbol{v}\|_{\mathrm{DG}} + h\|f - \pi_h f\|_{L^2(\Omega)} + h_\Lambda \|\hat{f} - \hat{\pi}_h \hat{f}\|_{L^2_A(\Lambda)} + h_B^{1/2} \|\overline{u} - \hat{u}\|_{L^2_P(\Lambda)}. \tag{4.20}$$

Proof. Here, we present the main steps of the proof. The details are given in the next section. We have, see Lemma 4.9 for the proof,

$$\|\boldsymbol{u} - \boldsymbol{u}_h\|_{\mathrm{DG}} \lesssim \inf_{\boldsymbol{v}\in\mathbb{V}_h^\Omega\times\mathbb{V}_h^\Lambda} \left(\|\boldsymbol{u} - \boldsymbol{v}\|_{\mathrm{DG}} + \sup_{\boldsymbol{\phi}\in\mathbb{V}_h^\Omega\times\mathbb{V}_h^\Lambda} \frac{(f, \phi - E\phi)_\Omega + (\hat{f}, \hat{\phi} - \hat{E}\hat{\phi})_{L^2_A(\Lambda)} - \mathcal{A}_h(\boldsymbol{v}, \boldsymbol{\phi} - \boldsymbol{E\phi})}{\|\boldsymbol{\phi}\|_{\mathrm{DG}}} \right). \tag{4.21}$$

We now bound the second term above. To this end, fix $\boldsymbol{v}, \boldsymbol{\phi} \in \mathbb{V}_h^\Omega \times \mathbb{V}_h^\Lambda$ and let $\boldsymbol{w} = \boldsymbol{\phi} - \boldsymbol{E\phi}$. Define $Z = (f, w)_\Omega + (\hat{f}, \hat{w})_{L^2_A(\Lambda)} - \mathcal{A}_h(\boldsymbol{v}, \boldsymbol{w})$. With the lift operator (4.14), we write

$$Z = (f - L_h v, w)_\Omega + (A\hat{f} - P\hat{L}_h\hat{v}, \hat{w})_\Lambda - a_h(v, w) - a_{\Lambda,h}(\hat{v}, \hat{w}). \tag{4.22}$$

We integrate by parts the first term in $a_h(v, w)$ and the first term in $a_{\Lambda,h}(\hat{v}, \hat{w})$. We obtain

$$Z = \underbrace{\sum_{K\in\mathcal{T}_\Omega^h} \int_K (f - L_h v + \Delta v) w + \sum_{i=1}^N \int_{s_{i-1}}^{s_i} (A\hat{f} - P\hat{L}_h\hat{v} + \mathrm{d}_s(A\,\mathrm{d}_s\hat{v}))\hat{w}}_{Z_1} \tag{4.23}$$

$$\underbrace{- \sum_{F\in\Gamma_h} \int_F [\nabla v]\cdot \boldsymbol{n}_F \{w\} - \sum_{i=0}^N [A\,\mathrm{d}_s\hat{v}]_{s_i}\{\hat{w}\}_{s_i}}_{Z_2} + Z_3 + Z_4,$$

where Z_3, Z_4 are the remaining terms in $a_h(v, w)$ and $a_{\Lambda,h}(\hat{v}, \hat{w})$ respectively. Namely,

$$Z_3 = -\epsilon_1 \sum_{F\in\Gamma_h\cup\partial\Omega} \int_F \{\nabla w\}\cdot \boldsymbol{n}_e [v] - \sum_{F\in\Gamma_h\cup\partial\Omega} \int_F \frac{\sigma_\Omega}{|F|^{1/2}} [v][w], \tag{4.24}$$

$$Z_4 = -\epsilon_2 \sum_{i=1}^{N-1} \{A\,\mathrm{d}_s\hat{w}\}_{s_i} [\hat{v}]_{s_i} - \sum_{i=1}^{N-1} \frac{\sigma_\Lambda}{h_\Lambda} [\hat{v}]_{s_i} [\hat{w}]_{s_i}. \tag{4.25}$$

We start by bounding Z_3 and Z_4. We note that $[u] = [E\phi] = 0$ a.e. on $F \in \Gamma_h \cup \partial\Omega$ and that $[\hat{u}]_{s_i} = [\hat{E}\hat{\phi}]_{s_i} = 0$, $i \in \{1, \dots N-1\}$. We use standard applications of trace inequality for polynomials and Cauchy-Schwarz's inequality, see for e.g. [28, Section 2.8.1] for a detailed exposition, to obtain

$$\begin{aligned} |Z_3| + |Z_4| &\lesssim \|w\|_{\mathbb{V}_h^\Omega} \|v - u\|_{\mathbb{V}_h^\Omega} + \|\hat{w}\|_{\mathbb{V}_h^\Lambda} \|\hat{v} - \hat{u}\|_{\mathbb{V}_h^\Lambda} \\ &\lesssim (\|\phi\|_{\mathbb{V}_h^\Omega} + |E\phi|_{H^1(\Omega)} + |\hat{\phi}|_{\mathbb{V}_h^\Lambda} + |\hat{E}\hat{\phi}|_{H^1(\Lambda)}) \|\boldsymbol{u} - \boldsymbol{v}\|_{\mathrm{DG}} \\ &\lesssim \|\boldsymbol{\phi}\|_{\mathrm{DG}} \|\boldsymbol{u} - \boldsymbol{v}\|_{\mathrm{DG}}. \end{aligned} \tag{4.26}$$

In the last inequality above, we used the stability of $\boldsymbol{E}$ given in (4.1) of Lemma 4.1, and the definition of $\|\cdot\|_{\mathrm{DG}}$. For the term Z_1, we use Cauchy–Schwarz's inequality and the approximation properties of $\boldsymbol{E}$ (4.2). We use the notation $\Lambda_i = (s_{i-1}, s_i)$ and we estimate

(4.27)
$$\begin{aligned}(Z_1)^2 &\leq \left(\sum_{K\in\mathcal{T}_\Omega^h} h_K^2\|f+\Delta v - L_h v\|^2_{L^2(K)} + \sum_{i=1}^N h_\Lambda^2 \|A\hat{f} + \mathrm{d}_s(A\,\mathrm{d}_s\hat{v}) - P\hat{L}_h\hat{v}\|^2_{L^2(\Lambda_i)}\right)\\ &\quad\times\left(\sum_{K\in\mathcal{T}_\Omega^h} h_K^{-2}\|w\|^2_{L^2(K)} + \sum_{i=1}^N h_\Lambda^{-2}\|\hat{w}\|^2_{L^2(\Lambda_i)}\right)\\ &\lesssim \left(\sum_{K\in\mathcal{T}_\Omega^h} h_K^2\|f+\Delta v - L_h v\|^2_{L^2(K)} + \sum_{i=1}^N h_\Lambda^2 \|A\hat{f} + \mathrm{d}_s(A\,\mathrm{d}_s\hat{v}) - P\hat{L}_h\hat{v}\|^2_{L^2(\Lambda_i)}\right)\|\boldsymbol{\phi}\|^2_{\mathrm{DG}}\\ &:= (R^1_\Omega + R^1_\Lambda)\|\boldsymbol{\phi}\|^2_{\mathrm{DG}}.\end{aligned}$$

For the term Z_2, first note that for $F = \partial K_F^1 \cap \partial K_F^2$ and $i = 1,\dots,N-1$, we use the following trace estimates [28, Section 2.1.3].

$$\|\{w\}\|_{L^2(F)} \lesssim |F|^{-1/4}\|w\|_{L^2(K_F^1\cup K_F^2)}, \quad |\{\hat{w}\}_{s_i}| \lesssim h_\Lambda^{-1/2}\|\hat{w}\|_{L^2(\Lambda_i\cup\Lambda_{i+1})}.$$

Applications of Cauchy–Schwarz's inequalities, the above estimates with the observation that $|F|^{-1/2}h_{K_F^j} \lesssim 1$ for $j = 1, 2$, and (4.2) yield

$$\begin{aligned}(Z_2)^2 &\lesssim \left(\sum_{F\in\Gamma_h} |F|^{1/2}\|[\nabla v]\cdot\boldsymbol{n}_F\|^2_{L^2(F)} + \sum_{i=0}^N h_\Lambda [A\,\mathrm{d}_s\hat{v}]^2_{s_i}\right)\\ &\quad\times\left(\sum_{K\in\mathcal{T}_\Omega^h} h_K^{-2}\|w\|^2_{L^2(K)} + \sum_{i=1}^N h_\Lambda^{-2}\|\hat{w}\|^2_{L^2(\Lambda_i)}\right)\\ &\lesssim \left(\sum_{F\in\Gamma_h} |F|^{1/2}\|[\nabla v]\cdot\boldsymbol{n}_F\|^2_{L^2(F)} + \sum_{i=0}^N h_\Lambda [A\,\mathrm{d}_s\hat{v}]^2_{s_i}\right)\|\boldsymbol{\phi}\|^2_{\mathrm{DG}} := (R^2_\Omega + R^2_\Lambda)\|\boldsymbol{\phi}\|^2_{\mathrm{DG}}.\end{aligned} \tag{4.28}$$

Combining the bounds above we have

$$\|\boldsymbol{u}-\boldsymbol{u}_h\|_{\mathrm{DG}} \leq \inf_{\boldsymbol{v}\in\mathbb{V}_h^\Omega\times\mathbb{V}_h^\Lambda}\left(\|\boldsymbol{u}-\boldsymbol{v}\|_{\mathrm{DG}} + (R^1_\Omega + R^1_\Lambda)^{1/2} + (R^2_\Omega + R^2_\Lambda)^{1/2}\right).$$

The proof is finished by obtaining the required bounds on the residual $(R^1_\Omega + R^1_\Lambda)$, see Lemma 4.10 and Corollary 4.11, and on the residual $(R^2_\Omega + R^2_\Lambda)$, see Lemma 4.12 and Corollary 4.13. ∎

Corollary 4.7 (Error rate). *Under the assumptions of Theorem 4.6, if $u \in H^{3/2-\eta}(\Omega)$ for any $\eta > 0$ and $\hat{u} \in H^2_A(\Lambda)$, then the following bound holds*

$$\|\boldsymbol{u}-\boldsymbol{u}_h\|_{\mathrm{DG}} \lesssim h^{1/2-\eta}(\|u\|_{H^{3/2-\eta}(\Omega)} + \|\overline{u}-\hat{u}\|_{L^2_P(\Lambda)} + \|f\|_{L^2(\Omega)}) + h_\Lambda(\|\hat{u}\|_{H^2_A(\Lambda)} + \|\hat{f}\|_{L^2_A(\Lambda)}). \tag{4.29}$$

Proof. Let $\boldsymbol{S}_h\boldsymbol{u} = (S_h u, \hat{S}_h\hat{u}) \in \mathbb{V}_h^\Omega \times \mathbb{V}_h^\Lambda$ where S_h and $\hat{S}_h$ are Scott–Zhang interpolants of u and $\hat{u}$ respectively [30]. With the triangle inequality, (2.8), and approximation properties, we bound

$$\begin{aligned}\|\boldsymbol{u}-\boldsymbol{S}_h\boldsymbol{u}\|_{\mathrm{DG}} &\lesssim \|u - S_h u\|_{H^1(\Omega)} + |\hat{u}-\hat{S}_h\hat{u}|_{H^1_A(\Lambda)} + \|\hat{u}-\hat{S}_h\hat{u}\|_{L^2_P(\Lambda)}\\ &\lesssim h^{1/2-\eta}\|u\|_{H^{3/2-\eta}(\Omega)} + h_\Lambda\|\hat{u}\|_{H^2_A(\Lambda)}.\end{aligned} \tag{4.30}$$

Using the above bound in (4.20) yields the desired estimate. ∎

We now show that if the mesh is refined near the boundary of B_Λ, (namely the mesh size is of the order h^{2k_1} where we recall k_1 is the polynomial degree for the space $\mathbb{V}_h^\Omega$) then almost optimal error estimates can be recovered. To this end, we use the definitions of graded meshes [2, 5, 19] in order to obtain the required estimates.

COROLLARY 4.8 (Graded meshes). *Let $r_K = \operatorname{dist}(K, \partial B_\Lambda)$ and recall that $h_K = \operatorname{diam}(K)$. Suppose that the mesh satisfies the following grading property.*

$$h_K \approx \begin{cases} h\, r_K^{1-\frac{1}{2k_1}}, & \text{if } r_K > \frac{1}{2}h_K, \\ h^{2k_1}, & \text{otherwise.} \end{cases} \tag{4.31}$$

Let $h_\Lambda \approx h_K$, for $K \in \mathcal{T}_B^h$. Assume that the assumptions of Theorem 4.6 hold. Further, assume that $u \in H^{k_1+1}(\Omega\backslash\overline{B_\Lambda}) \cap H^{k_1+1}(B_\Lambda)$, $\hat{u} \in H^2(\Lambda)$, $f \in H^{k_1-1}(\Omega)$, and $\hat{f} \in L^2(\Lambda)$. Then,

$$\begin{aligned} \|\boldsymbol{u} - \boldsymbol{u}_h\|_{\mathrm{DG}} \lesssim & h^{k_1-2\eta}(\|u\|_{H^{k_1+1}(B_\Lambda)} + \|u\|_{H^{k_1+1}(\Omega\backslash\overline{B_\Lambda})} + \|u\|_{H^{3/2-\eta}(\Omega)} + \|f\|_{H^{k_1-1}(\Omega)}) \\ & + h^{2k_1}(\|\hat{u}\|_{H^2(\Lambda)} + \|\hat{f}\|_{L^2(\Lambda)}). \end{aligned} \tag{4.32}$$

Proof. Define an interpolant $I_h u \in \mathbb{V}_h^\Omega$ such that $I_h u|_K = S_h u|_K$, the Scott–Zhang interpolant restricted to K, if $r_K \le \frac{1}{2}h_K$ and $I_h u|_K = \pi_h u$, the local L^2 projection, otherwise. We use the local approximation properties of the Scott–Zhang interpolant. Namely, we have that [30]

$$|u - S_h u|_{H^1(K)} + h_K^{-1}\|u - S_h u\|_{L^2(K)} \lesssim h_K^{\min(k_1+1,s)-1}\|u\|_{H^s(\Delta_K)}, \quad 1 \le s \le k_1 + 1. \tag{4.33}$$

In the above, Δ_K is the union of elements sharing a face with K. Hence, we obtain that

$$\begin{aligned} \sum_{K\in\mathcal{T}_\Omega^h, r_K \le \frac{1}{2}h_K} & \left(|u - I_h u|_{H^1(K)}^2 + h_K^{-2}\|u - I_h u\|_{L^2(K)}^2\right) \\ & \lesssim \sum_{K\in\mathcal{T}_\Omega^h, r_K \le \frac{1}{2}h_K} h_K^{1-2\eta}\|u\|_{H^{3/2-\eta}(\Delta_K)}^2 \lesssim h^{2k_1(1-2\eta)}\|u\|_{H^{3/2-\eta}(\Omega)}^2. \end{aligned} \tag{4.34}$$

Further, using the approximation properties of the L^2 projection, we obtain

$$\begin{aligned} \sum_{K\in\mathcal{T}_\Omega^h, r_K > \frac{1}{2}h_K} & \left(|u - I_h u|_{H^1(K)}^2 + h_K^{-2}\|u - I_h u\|_{L^2(K)}^2\right) \\ & \lesssim \sum_{K\in\mathcal{T}_\Omega^h, r_K > \frac{1}{2}h_K} h^{2k_1}\|u\|_{H^{k_1+1}(K)}^2 \lesssim h^{2k_1}(\|u\|_{H^{k_1+1}(B_\Lambda)}^2 + \|u\|_{H^{k_1+1}(\Omega\backslash\overline{B_\Lambda})}^2). \end{aligned} \tag{4.35}$$

In the above, we also used that $r_K \lesssim \operatorname{diam}(\Omega)$. Now, note that

$$\|u - I_h u\|_{\mathbb{V}_h^\Omega}^2 \lesssim \sum_{K\in\mathcal{T}_\Omega^h} \left(|u - I_h u|_{H^1(K)}^2 + h_K^{-2}\|u - I_h u\|_{L^2(K)}^2\right). \tag{4.36}$$

Define $\boldsymbol{I}_h\boldsymbol{u} = (I_h u, \hat{S}_h\hat{u})$. We use the above bounds, triangle inequality, (4.8), and approximation properties of $\hat{S}_h$ to obtain that

$$\begin{aligned} \|\boldsymbol{u} - \boldsymbol{I}_h\boldsymbol{u}\|_{\mathrm{DG}} & \lesssim \|u - I_h u\|_{\mathbb{V}_h^\Omega} + |\hat{u} - \hat{S}_h\hat{u}|_{\mathbb{V}_h^\Lambda} + \|\hat{u} - \hat{S}_h\hat{u}\|_{L_P^2(\Lambda)} \\ & \lesssim h^{k_1}(\|u\|_{H^{k_1+1}(B_\Lambda)} + \|u\|_{H^{k_1+1}(\Omega\backslash\overline{B_\Lambda})} + h^{-2\eta}\|u\|_{H^{3/2-\eta}(\Omega)}) + h^{2k_1}\|\hat{u}\|_{H^2(\Lambda)}. \end{aligned} \tag{4.37}$$

In the above, we used the assumption that $h_\Lambda \approx h_K$ for $K \in \mathcal{T}_B^h$ and thus $h_\Lambda \approx h^{2k_1}$. The above bound estimates the first term of (4.20). The second and third terms in (4.20) are bounded by the approximation properties of the L^2 projections, see (4.4). Finally, the last term in (4.20) is controlled by observing that $r_K \lesssim \frac{1}{2}h_K$, $\forall K \in \mathcal{T}_B^h$. Thus, using (4.31), $h_B \lesssim h^{2k_1}$. Along with (2.8), this concludes the proof. ∎

4.3. Proof details. We now provide details for the steps given in the proof of Theorem 4.6.

LEMMA 4.9. *Let* $\boldsymbol{u}$ *and* $\boldsymbol{u}_h$ *be the solutions of* (2.15) *and* (3.14) *respectively. Then,* (4.21) *holds.*

Proof. The proof follows from the abstract framework given in [16, Lemma 2.1]. In the notation of this Lemma, we set $V = H^1_0(\Omega) \times H^1_A(\Lambda)$, $\|\boldsymbol{v}\|^2_V = \|v\|^2_{H^1(\Omega)} + \|v\|^2_{H^1_A(\Lambda)}$, and $\|\cdot\|_h = \|\cdot\|_{\mathrm{DG}}$. We verify assumptions (N1)–(N3) of [16]. Observe that assumption (N1) is the coercivity estimate of Lemma 3.1. We now verify assumption (N3) which states that

$$\|\boldsymbol{E}\boldsymbol{v}\|_V \lesssim \|\boldsymbol{v}\|_{\mathrm{DG}}, \quad \forall \boldsymbol{v} \in \mathbb{V}^\Omega_h \times \mathbb{V}^\Lambda_h. \tag{4.38}$$

Let $\boldsymbol{v} = (v, \hat{v}) \in \mathbb{V}^\Omega_h \times \mathbb{V}^\Lambda_h$. From Lemma 4.1, we have

$$\|Ev\|_{H^1(\Omega)} + \|\hat{E}\hat{v}\|_{H^1_A(\Lambda)} \lesssim \|v\|_{L^2(\Omega)} + \|\hat{v}\|_{L^2_A(\Lambda)} + \|v\|_{\mathbb{V}^\Omega_h} + |\hat{v}|_{\mathbb{V}^\Lambda_h}. \tag{4.39}$$

For the first term above, we use Poincaré's inequality (3.9). For the second term, we use the fact that $A, P > 0$, triangle inequality, and trace inequality (Lemma 4.4):

$$\|\hat{v}\|_{L^2_A(\Lambda)} \lesssim \|\hat{v} - \overline{v}\|_{L^2_P(\Lambda)} + \|\overline{v}\|_{L^2_P(\Lambda)} \lesssim \|\hat{v} - \overline{v}\|_{L^2_P(\Lambda)} + \|v\|_{\mathbb{V}^\Omega_h}. \tag{4.40}$$

Therefore, we obtain that

$$\|Ev\|_{H^1(\Omega)} + \|\hat{E}\hat{v}\|_{H^1_A(\Lambda)} \lesssim \|v\|_{\mathbb{V}^\Omega_h} + \|\hat{v}\|_{\mathbb{V}^\Lambda_h} + \|\overline{v} - \hat{v}\|_{L^2_P(\Lambda)} \lesssim \|\boldsymbol{v}\|_{\mathrm{DG}}. \tag{4.41}$$

Hence, (4.38) is verified. It remains to verify (N2). We show that for $\boldsymbol{v} \in H^1_0(\Omega) \times H^1(\Lambda)$, $\boldsymbol{v}_h \in \mathbb{V}^\Omega_h \times \mathbb{V}^\Lambda_h$, and $\boldsymbol{w} \in \mathbb{V}^\Omega_{h,c} \times \mathbb{V}^\Lambda_{h,c}$, there holds

$$\mathcal{A}(\boldsymbol{v}, \boldsymbol{w}) - \mathcal{A}_h(\boldsymbol{v}_h, \boldsymbol{w}) \lesssim \|\boldsymbol{v} - \boldsymbol{v}_h\|_{\mathrm{DG}} (\|w\|^2_{H^1(\Omega)} + \|\hat{w}\|^2_{H^1_A(\Lambda)})^{1/2}. \tag{4.42}$$

For this, observe that $[v] = [w] = 0$ a.e. on $e \in \Gamma_h \cup \partial\Omega$. Thus, we have that

$$a(v, w) - a_h(v_h, w) = \sum_{K \in \mathcal{T}^h_\Omega} \int_K \nabla(v - v_h) \cdot \nabla w - \epsilon_1 \sum_{F \in \Gamma_h \cup \partial\Omega} \int_F \{\nabla w\} \cdot \boldsymbol{n}_F [v_h - v].$$

With the trace estimate for polynomials

$$|F|^{1/4} \|\{\nabla w\} \cdot \boldsymbol{n}_F\|_{L^2(F)} \lesssim \|\nabla w\|_{L^2(K^1_F \cup K^2_F)}, \quad F = \partial K^1_F \cap \partial K^2_F,$$

and Cauchy-Schwarz's inequality, we obtain that

$$a(v, w) - a_h(v_h, w) \lesssim \|v_h - v\|_{\mathbb{V}^\Omega_h} |w|_{H^1(\Omega)}. \tag{4.43}$$

A similar argument shows that

$$a_\Lambda(\hat{v}, \hat{w}) - a_{\Lambda,h}(\hat{v}_h, \hat{w}) \lesssim |\hat{v}_h - \hat{v}|_{\mathbb{V}^\Lambda_h} |\hat{w}|_{H^1_A(\Lambda)}. \tag{4.44}$$

For the remainder terms, we simply use Cauchy-Schwarz's inequality and the trace estimate (2.8). Indeed, we have that

$$\begin{aligned} b_\Lambda(\overline{v} - \hat{v}, \overline{w} - \hat{w}) - b_\Lambda(\overline{v}_h - \hat{v}_h, \overline{w} - \hat{w}) &\le \xi \|\overline{v} - \overline{v}_h - (\hat{v} - \hat{v}_h)\|_{L^2_P(\Lambda)} \|\overline{w} - \hat{w}\|_{L^2_P(\Lambda)} \\ &\lesssim \|\boldsymbol{v} - \boldsymbol{v}_h\|_{\mathrm{DG}} (\|w\|_{H^1(\Omega)} + \|\hat{w}\|_{L^2_P(\Lambda)}) \lesssim \|\boldsymbol{v} - \boldsymbol{v}_h\|_{\mathrm{DG}} (\|w\|_{H^1(\Omega)} + \|\hat{w}\|_{H^1_A(\Lambda)}). \end{aligned}$$

Estimate (4.42) follows by combining the above bounds. The proof is finished by applying [16, Lemma 2.1]. ∎

We now show the first residual bound. We recall that for any $K \in \mathcal{T}^h_B$, the set $\mathcal{I}_K$ denotes the set of integers i_0 such that $K \in \omega_{i_0}$.

LEMMA 4.10 (Bound on local residuals over elements). *Fix $1 \le i \le N$ and recall that $\Lambda_i = (s_{i-1}, s_i)$. For all $v_h \in \mathbb{V}_h^\Omega$ and any $K \in \omega_i$, there holds*

$$\|f + \Delta v - L_h v\|^2_{L^2(K)} \lesssim h_K^{-2}\|\nabla(u-v)\|_{L^2(K)} + h_K^{-1}\sum_{j\in\mathcal{I}_K}\|\overline{u}-\hat{u}\|^2_{L^2_P(\Lambda_j)} + \|L_h(u-v)\|^2_{L^2(K)} + \|\pi_h f - f\|^2_{L^2(K)}. \tag{4.45}$$

For any $\hat{v}_h \in \mathbb{V}_h^\Lambda$, there holds

$$\|A\hat{f} + \mathrm{d}_s(A\,\mathrm{d}_s\hat{v}) - P\hat{L}_h\hat{v}\|^2_{L^2(\Lambda_i)} \lesssim h_\Lambda^{-2}\|\mathrm{d}_s(\hat{u}-\hat{v})\|^2_{L^2_A(\Lambda_i)} + \|\overline{u}-\hat{u}\|^2_{L^2_P(\Lambda_i)} + \|\hat{L}_h(\hat{u}-\hat{v})\|^2_{L^2_P(\Lambda_i)} + \|\hat{\pi}_h\hat{f}-\hat{f}\|^2_{L^2_A(\Lambda_i)}. \tag{4.46}$$

Proof. Let b_K be the bubble function associated to K [31]. Define the residuals $R = (\pi_h f + \Delta v - L_h v)|_K$ and $\psi = R\,b_K$. Owing to the properties of the bubble functions, we estimate

$$\|R\|^2_{L^2(K)} \lesssim \int_K R\psi = \int_K (f + \Delta v - L_h v)\psi + \int_K (\pi_h f - f)\psi = T_1 + T_2.$$

Since ψ vanishes on the boundary of K, we integrate by parts and obtain

$$T_1 = \int_K (f\psi - \nabla v\cdot\nabla\psi - L_h v\,\psi). \tag{4.47}$$

Testing (2.15) with $(\psi, 0)$ and substituting in the above gives

$$T_1 = \int_K \nabla(u-v)\cdot\nabla\psi + b_\Lambda(\overline{u}-\hat{u}, \overline{\psi}) - \int_K L_h v\,\psi. \tag{4.48}$$

The first term is bounded by Cauchy-Schwarz's inequality and inverse estimates since ψ belongs to a finite dimensional space.

$$T_1 \lesssim h_K^{-1}\|\nabla(u-v)\|_{L^2(K)}\|\psi\|_{L^2(K)} + b_\Lambda(\overline{u}-\hat{u}, \overline{\psi}) - \int_K L_h v\,\psi.$$

For the second term above, we use the definition of the lift operator (4.14) and write

$$b_\Lambda(\overline{u}-\hat{u}, \overline{\psi}) = b_\Lambda(\overline{u}-\hat{u}, \overline{\psi} - \overline{\pi_h\psi}) + (L_h u, \pi_h\psi)_K = b_\Lambda(\overline{u}-\hat{u}, \overline{\psi} - \overline{\pi_h\psi}) + (L_h u, \psi)_K.$$

Here we used the definition of the L^2 projections in (4.3) and the fact that $L_h u \in \mathbb{V}_h^\Omega$. Since ψ is locally supported on one element K, with Cauchy–Schwarz's inequality, trace estimate (4.7), and stability of the L^2 projection, we obtain the bound

$$\sum_{j\in\mathcal{I}_K}\|\overline{\psi} - \overline{\pi_h\psi}\|^2_{L^2_P(\Lambda_j)} \le \|\psi - \pi_h\psi\|^2_{L^2(\partial B_\Lambda\cap K)} \lesssim h_K^{-1}\|\psi - \pi_h\psi\|^2_{L^2(K)} \lesssim h_K^{-1}\|\psi\|^2_{L^2(K)}.$$

Thus, with Cauchy-Schwarz's and triangle inequalities, we obtain that

$$b_\Lambda(\overline{u}-\hat{u}, \overline{\psi} - \overline{\pi_h\psi}) \lesssim h_K^{-1/2}\Big(\sum_{j\in\mathcal{I}_K}\|\overline{u}-\hat{u}\|^2_{L^2_P(\Lambda_j)}\Big)^{1/2}\|\psi\|_{L^2(K)}. \tag{4.49}$$

Thus, we obtain

$$T_1 \lesssim \|\psi\|_{L^2(K)}\left(h_K^{-1}\|\nabla(u-v)\|_{L^2(K)} + \|L_h(u-v)\|_{L^2(K)} + h_K^{-1/2}\Big(\sum_{j\in\mathcal{I}_K}\|\overline{u}-\hat{u}\|^2_{L^2_P(\Lambda_j)}\Big)^{1/2}\right).$$

The term T_2 is simply handled by Cauchy-Schwarz's inequality. Collecting the resulting bounds in (11), noting that $\|\psi\|_{L^2(K)} \lesssim \|R\|_{L^2(K)}$, and using the triangle inequality yields estimate (4.45).

To show (4.46), let $\hat{b}_i$ denote the bubble functions associated to Λ_i, $\hat{R} = (A\hat{\pi}_h\hat{f} + \mathrm{d}_s(A\,\mathrm{d}_s\hat{v}) - P\hat{L}_h\hat{v})|_{\Lambda_i}$, and $\hat{\psi} = \hat{R}\hat{b}_i$. We have

$$\|\hat{R}\|^2_{L^2(\Lambda_i)} \lesssim \int_{\Lambda_i} \hat{R}\hat{\psi} = \int_{\Lambda_i} (A\hat{f} + \mathrm{d}_s(A\,\mathrm{d}_s\hat{v}) - P\hat{L}_h\hat{v})\hat{\psi} + \int_{\Lambda_i} A(\hat{\pi}_h\hat{f} - \hat{f})\hat{\psi} = T_3 + T_4.$$

Testing (2.15) with $(0, \hat{\psi})$ and performing the same computation as before, we obtain

$$T_3 = \int_{\Lambda_i} A\,\mathrm{d}_s(\hat{u} - \hat{v})\,\mathrm{d}_s\hat{\psi} - b_\Lambda(\overline{u} - \hat{u}, \hat{\psi} - \hat{\pi}_h\hat{\psi}) + \int_{\Lambda_i} P\hat{L}_h(\hat{u} - \hat{v})\hat{\psi}. \tag{4.50}$$

With Cauchy–Schwarz's and inverse inequalities, the stability of the L^2 projection, and the fact that $\hat{\psi}$ is locally supported in Λ_i, we obtain

$$T_3 \lesssim \|\hat{\psi}\|_{L^2_P(\Lambda_i)}(h_\Lambda^{-1}\|\mathrm{d}_s(\hat{u} - \hat{v})\|_{L^2_A(\Lambda_i)} + \|\hat{L}_h(\hat{u} - \hat{v})\|_{L^2_P(\Lambda_i)} + \|\overline{u} - \hat{u}\|_{L^2_P(\Lambda_i)}).$$

Bounding T_4 with Cauchy–Schwarz's inequality and using that $\|\hat{\psi}\|_{L^2_P(\Lambda_i)} \lesssim \|\hat{R}\|_{L^2(\Lambda_i)}$, estimate (4.46) is obtained. ∎

An immediate corollary to the above Lemmas is the following global bound.

Corollary 4.11. *Recall that $h_B = \max_{K\in\mathcal{T}_B^h} h_K$. The following bound on $R^1_\Omega + R^1_\Lambda$ (as defined in (4.27)) holds.*

$$\begin{aligned}(R^1_\Omega + R^1_\Lambda) \lesssim &\|\boldsymbol{u} - \boldsymbol{v}\|^2_{\mathrm{DG}} + (h_B + h_\Lambda^2)\|\overline{u} - \hat{u}\|^2_{L^2_P(\Lambda)} \\ &+ h^2\|f - \pi_h f\|^2_{L^2(\Omega)} + h_\Lambda^2\|\hat{f} - \hat{\pi}_h\hat{f}\|_{L^2_A(\Lambda)}.\end{aligned} \tag{4.51}$$

Proof. First note that if $K \notin \mathcal{T}_B^h$, then $L_h v = 0$ on K, and $\mathcal{I}_K = \emptyset$. We can write

$$R^1_\Omega = \sum_{K\in\mathcal{T}_B^h} h_K^2\|f + \Delta v - L_h v\|^2_{L^2(K)} + \sum_{K\in\mathcal{T}_\Omega^h\setminus\mathcal{T}_B^h} h_K^2\|f + \Delta v\|^2_{L^2(K)}.$$

For the first term in the right-hand side, we use Lemma 4.10 and the assumption that $|\mathcal{I}_K| \lesssim C$ for all $K \in \mathcal{T}_B^h$ to obtain the bound:

$$\begin{aligned}R^1_\Omega \lesssim &\|u - v\|^2_{\mathbb{V}_h^\Omega} + h_B\|\overline{u} - \hat{u}\|^2_{L^2_P(\Lambda)} + h^2\|f - \pi_h f\|^2_{L^2(\Omega)} \\ &+ \sum_{K\in\mathcal{T}_B^h} h_K^2\|L_h(u - v)\|^2_{L^2(K)} + \sum_{K\in\mathcal{T}_\Omega^h\setminus\mathcal{T}_B^h} h_K^2\|f + \Delta v\|^2_{L^2(K)}.\end{aligned}$$

If $K \notin \mathcal{T}_B^h$, then standard a posteriori estimates [7, Section 5.5.1] yield

$$h_K^2\|f + \Delta v\|^2_{L^2(K)} \lesssim \|\nabla(u - v)\|^2_{L^2(K)} + h_K^2\|f - \pi_h f\|^2_{L^2(K)},\ \forall K \in \mathcal{T}_\Omega^h \setminus \mathcal{T}_B^h.$$

With the bound above and Lemma 4.5, we can conclude that bound (4.51) holds on R^1_Ω. The same bound holds on R^1_Λ which follows immediately from Lemma 4.10 and Lemma 4.5. ∎

We proceed to bound on $R^2_\Omega + R^2_\Lambda$. For any face F, let $S_F = K^1_F \cup K^2_F$ where K^1_F and K^2_F are the elements sharing the face F. We also define

$$\forall 1 \le i \le N-1, \quad \hat{S}_i = \Lambda_{i-1} \cup \Lambda_i, \quad \hat{S}_0 = \Lambda_0, \quad \hat{S}_N = \Lambda_{N-1}, \quad \hat{S}_{N+1} = \emptyset.$$

LEMMA 4.12 (Bound on local residual over faces). *Fix $1 \le i \le N$. Then, for any $F \in \Gamma_i$, and any $v \in \mathbb{V}_h^\Omega$, there holds*

$$\|[\nabla v]\cdot \boldsymbol{n}_F\|^2_{L^2(F)} \lesssim |F|^{-1/2} \sum_{K\subset S_F} \|\nabla(u-v)\|^2_{L^2(K)} + |F|^{1/2} \sum_{K\subset S_F} \|f+\Delta v - L_h v\|^2_{L^2(K)} + |F|^{1/2}\|L_h(u-v)\|^2_{L^2(S_F)} + \|\overline{u}-\hat{u}\|^2_{L^2_P(\hat{S}_i\cup\hat{S}_{i+1})}. \tag{4.52}$$

For any $\hat{v} \in \mathbb{V}_h^\Lambda$, there holds

$$[A\,\mathrm{d}_s\hat{v}]^2_{s_i} \lesssim h_\Lambda^{-1}\|\mathrm{d}_s(\hat{u}-\hat{v})\|^2_{L^2_A(\hat{S}_i)} + h_\Lambda \sum_{\Lambda_\ell\subset\hat{S}_i} \|A\hat{f} + \mathrm{d}_s(A\,\mathrm{d}_s\hat{v}) - PL_h\hat{v}\|^2_{L^2(\Lambda_\ell)} + h_\Lambda\|\hat{L}_h(\hat{u}-\hat{v})\|^2_{L^2(\hat{S}_i)} + h_\Lambda\|\overline{u}-\hat{u}\|^2_{L^2_P(\hat{S}_i)}. \tag{4.53}$$

Proof. Fix $1 \le i \le N$ and fix F in Γ_i. Denote by b_F the face bubble associated to F; this means that b_F vanishes on the boundary of S_F and b_F takes the value one at the barycenter of F. Fix v in $\mathbb{V}_h^\Omega$. We set $r = [\nabla v]\cdot\boldsymbol{n}_F$, extend r by constant values along $\boldsymbol{n}_F$, and set $\psi = rb_F$. From [7, proof of Lemma 5.7 (ii)], we have

$$\|\psi\|_{L^2(S_F)} \lesssim |F|^{1/4}\|r\|_{L^2(F)}. \tag{4.54}$$

With the properties of the bubble function and integration by parts, we have

$$\|r\|^2_{L^2(F)} \lesssim \int_F r\psi = \int_F [\nabla v]\cdot\boldsymbol{n}_F\psi = \sum_{K\subset S_F}\int_K \Delta v\,\psi + \sum_{K\subset S_F}\int_K \nabla v\cdot\nabla\psi. \tag{4.55}$$

Choose the test function $\boldsymbol{v} = (\psi, 0)$ in (2.15)

$$\sum_{K\subset S_F}\int_K \nabla u\cdot\nabla\psi + b_\Lambda(\overline{u}-\hat{u},\overline{\psi}) = \int_{S_F} f\psi. \tag{4.56}$$

We introduce the L^2 projection and rewrite the second term above as

$$b_\Lambda(\overline{u}-\hat{u},\overline{\psi}) = b_\Lambda(\overline{u}-\hat{u},\overline{\psi}-\overline{\pi_h\psi}) + (L_h u,\pi_h\psi)_\Omega = b_\Lambda(\overline{u}-\hat{u},\overline{\psi}-\overline{\pi_h\psi}) + \int_{S_F} L_h u\,\psi.$$

We add (4.56) to (4.55), use the above expansion, and add and subtract $L_h v$. We obtain

$$\|r\|^2_{L^2(F)} \lesssim \sum_{K\subset S_F}\int_K (f+\Delta v - L_h v)\psi + \int_{S_F} L_h(v-u)\,\psi + \sum_{K\subset S_F}\int_K \nabla(v-u)\cdot\nabla\psi - b_\Lambda(\overline{u}-\hat{u},\overline{\psi}-\overline{\pi_h\psi}) = W_1+\ldots+W_4.$$

With (4.54), the terms W_1 and W_2 are bounded as:

$$W_1+W_2 \lesssim |F|^{1/4}\|r\|_{L^2(F)}\left((\sum_{K\subset S_F}\|f+\Delta v - L_h v\|^2_{L^2(K)})^{1/2} + \|L_h(u-v)\|_{L^2(S_F)}\right).$$

With inverse estimates and (4.54) and the observation that $h^{-1}_{K_F^\ell}|F|^{1/4} \lesssim |F|^{-1/4}$ for $\ell = 1,2$, we bound

$$W_3 \lesssim |F|^{-1/4}\|r\|_{L^2(F)}(\sum_{K\subset S_F}\|\nabla(u-v)\|^2_{L^2(K)})^{1/2}.$$

Let K_F^1 and K_F^2 denote the elements that share the face F and let $\mathcal{J}_F$ denote the set of indices i_0 such that K_F^1 belongs to ω_{i_0} or such that K_F^2 belongs to ω_{i_0}. In reality, the set $\mathcal{J}_F$ is either the

singleton $\{i\}$ (recall that F belongs to Γ_i) or the pair $\{i, i+1\}$ or the pair $\{i-1, i\}$ or the triplet $\{i-1, i, i+1\}$.

$$\begin{aligned} W_4 = (\xi P(\overline{u}-\hat{u}), \overline{\psi} - \overline{\pi_h\psi})_\Lambda &= \sum_{\ell\in\mathcal{J}_F} (\xi P(\overline{u}-\hat{u}), \overline{\psi} - \overline{\pi_h\psi})_{\Lambda_\ell} \\ &\le \xi(\sum_{\ell\in\mathcal{J}_F} \|\overline{u}-\hat{u}\|^2_{L^2_P(\Lambda_\ell)})^{1/2} (\sum_{\ell\in\mathcal{J}_F} \|\overline{\psi} - \overline{\pi_h\psi}\|^2_{L^2_P(\Lambda_\ell)})^{1/2} \\ &\le \xi(\sum_{\ell\in\mathcal{J}_F} \|\overline{u}-\hat{u}\|^2_{L^2_P(\Lambda_\ell)})^{1/2} \|\psi - \pi_h\psi\|_{L^2(S_F\cap\partial B_\Lambda)}. \end{aligned}$$

With Cauchy-Schwarz inequality and trace estimate (4.7), we obtain

$$\begin{aligned} W_4 &\lesssim \xi(\sum_{\ell\in\mathcal{J}_F} \|\overline{u}-\hat{u}\|^2_{L^2(\Lambda_\ell)})^{1/2} (\sum_{K\subset S_F} h_K^{-1}\|\psi-\pi_h\psi\|^2_{L^2(K)})^{1/2} \\ &\lesssim h_F^{-1/2}\|\overline{u}-\hat{u}\|_{L^2(\hat{S}_i\cup\hat{S}_{i+1})}\|\psi\|_{L^2(S_F)}, \end{aligned}$$

where $h_F = \min(h_{K_F^1}, h_{K_F^2})$. Therefore, with (4.54), we have

$$W_4 \lesssim h_F^{-1/2}|F|^{1/4}\|r\|_{L^2(F)}\|\overline{u}-\hat{u}\|_{L^2(\hat{S}_i\cup\hat{S}_{i+1})} \lesssim \|r\|_{L^2(F)}\|\overline{u}-\hat{u}\|_{L^2(\hat{S}_i\cup\hat{S}_{i+1})}. \tag{4.57}$$

Collecting the above bounds and using appropriate Young's inequalities yield (4.52). To prove the bound (4.53), we denote by $\hat{b}_i$ the typical hat function associated to the node s_i; this means that $\hat{b}_i$ is piecewise linear, takes the value 1 at s_i and the value 0 at all the other nodes s_ℓ for $\ell \neq i$. Denote by $\hat{r}_i = [A\,\mathrm{d}_s\hat{v}]_{s_i}$ and let $\hat{\psi}_i = \hat{r}_i\hat{b}_i$. It easily follows that

$$\|\hat{\psi}_i\|_{L^2(\hat{S}_i)} \lesssim h_\Lambda^{1/2}|\hat{r}_i|. \tag{4.58}$$

Using integration by parts, it is easy to check that

$$\hat{r}_i^2 = [A\,\mathrm{d}_s\hat{v}]_{s_i}\hat{\psi}_i(s_i) = \sum_{\Lambda_\ell\subset\hat{S}_i} \left(\int_{\Lambda_\ell} \mathrm{d}_s(A\,\mathrm{d}_s\hat{v})\,\hat{\psi}_i + \int_{\Lambda_\ell} A\,\mathrm{d}_s\hat{v}\,\mathrm{d}_s\hat{\psi}_i \right). \tag{4.59}$$

This time, we choose for test function $\boldsymbol{v} = (0, \hat{\psi}_i)$ in (2.15) to obtain

$$\sum_{\Lambda_\ell\subset\hat{S}_i} \int_{\Lambda_\ell} A\,\mathrm{d}_s\hat{u}\;\mathrm{d}_s\hat{\psi}_i - b_\Lambda(\overline{u}-\hat{u}, \hat{\psi}_i) = \int_{\hat{S}_i} A\hat{f}\hat{\psi}_i. \tag{4.60}$$

We rewrite it as

$$\sum_{\Lambda_\ell\subset\hat{S}_i} \int_{\Lambda_\ell} A\,\mathrm{d}_s\hat{u}\;\mathrm{d}_s\hat{\psi}_i - b_\Lambda(\overline{u}-\hat{u}, \hat{\psi}_i - \hat{\pi}_h\hat{\psi}_i) + \int_{\hat{S}_i} P\hat{L}_h\hat{u}\,\hat{\psi}_i = \int_{\hat{S}_i} A\hat{f}\hat{\psi}_i. \tag{4.61}$$

We add (4.61) to (4.59) and we add and subtract $P\hat{L}_h\hat{v}$. We obtain

$$\begin{aligned} \hat{r}_i^2 \lesssim &\sum_{\Lambda_\ell\subset\hat{S}_i} \int_{\Lambda_\ell} (A\hat{f} + \mathrm{d}_s(A\,\mathrm{d}_s\hat{v}) - P\hat{L}_h\hat{v})\hat{\psi}_i + \int_{\hat{S}_i} P\hat{L}_h(\hat{v}-\hat{u})\hat{\psi}_i \\ &+ \sum_{\Lambda_\ell\subset\hat{S}_i} \int_{\Lambda_\ell} A\,\mathrm{d}_s(\hat{v}-\hat{u})\,\mathrm{d}_s\hat{\psi}_i + b_\Lambda(\overline{u}-\hat{u}, \hat{\psi}_i - \hat{\pi}_h\hat{\psi}_i) = W_5 + \ldots + W_8. \end{aligned}$$

We easily bound the terms W_5, W_6 and W_7 by (4.58)

$$\begin{aligned} W_5 + W_6 &\lesssim h_\Lambda^{1/2}|\hat{r}_i| \left((\sum_{\Lambda_\ell\subset\hat{S}_i} \|A\hat{f} + \mathrm{d}_s(A\,\mathrm{d}_s\hat{v}) - P\hat{L}_h\hat{v}\|^2_{L^2(\Lambda_\ell)})^{1/2} + \|\hat{L}_h(\hat{u}-\hat{v})\|_{L^2_P(\hat{S}_i)} \right), \\ W_7 &\lesssim h_\Lambda^{-1/2}|\hat{r}_i| (\sum_{\Lambda_\ell\subset\hat{S}_i} \|\mathrm{d}_s(\hat{u}-\hat{v})\|^2_{L^2_A(\Lambda_\ell)})^{1/2}. \end{aligned}$$

For the term W_8, we have by Cauchy-Schwarz and stability of the L^2–projection that

$$W_8 \lesssim \|\overline{u}-\hat{u}\|_{L^2_P(\hat{S}_i)}\|\hat{\psi}_i-\hat{\pi}_h\hat{\psi}_i\|_{L^2_P(\hat{S}_i)} \lesssim \|\overline{u}-\hat{u}\|_{L^2_P(\hat{S}_i)}\|\hat{\psi}_i\|_{L^2_P(\hat{S}_i)} \lesssim h_\Lambda^{1/2}\|\overline{u}-\hat{u}\|_{L^2_P(\hat{S}_i)}|\hat{r}_i|.$$

Collecting the above bounds yield the desired result. ∎

The bound on $(R_\Omega^2+R_\Lambda^2)$ easily follows.

COROLLARY 4.13. *The following bound on $R_\Omega^2+R_\Lambda^2$ as defined in (4.28) holds.*

$$\begin{aligned}(R_\Omega^2+R_\Lambda^2) \lesssim & \|\boldsymbol{u}-\boldsymbol{v}\|_{\mathrm{DG}}^2+(h_B+h_\Lambda^2)\|\overline{u}-\hat{u}\|^2_{L^2_P(\Lambda)}\\ &+h^2\|f-\pi_h f\|^2_{L^2(\Omega)}+h_\Lambda^2\|\hat{f}-\hat{\pi}_h\hat{f}\|_{L^2_A(\Lambda)}.\end{aligned} \tag{4.62}$$

Proof. Recalling the definition of (3.5), we have

$$R_\Omega^2=\sum_{i=1}^N\sum_{F\in\Gamma_i}|F|^{1/2}\|[\nabla v]\cdot\boldsymbol{n}_F\|^2_{L^2(F)}+\sum_{F\in\Gamma_h\setminus\bigcup_{i=1}^N\Gamma_i}|F|^{1/2}\|[\nabla v]\cdot\boldsymbol{n}_F\|^2_{L^2(F)}.$$

The first part is bounded using Lemma 4.12.

$$\begin{aligned}\sum_{i=1}^N\sum_{F\in\Gamma_i}|F|^{1/2}\|[\nabla v]\cdot\boldsymbol{n}_F\|^2_{L^2(F)} \lesssim & \|u-v\|^2_{\mathbb{V}_h^\Omega}\\ &+\sum_{K\in\mathcal{T}_\Omega^h}h_K^2(\|f+\Delta v-L_hv\|^2_{L^2(K)}+\|L_h(u-v)\|^2_{L^2(K)})+h_B^2\|\overline{u}-\hat{u}\|^2_{L^2_P(\Lambda)}.\end{aligned}$$

If F does not belong to $\bigcup_{i=1}^N\Gamma_i$, then $L_hv=0$ on S_F and standard a posteriori estimates are used. We omit the details for brevity. Following [7, Lemma 5.27], we have

$$|F|^{1/2}\|[\nabla v]\cdot\boldsymbol{n}_F\|^2_{L^2(F)}\lesssim\sum_{K\subset S_F}\|\nabla(u-v)\|^2_{L^2(K)}+h_{S_F}^2\|f-\pi_hf\|^2_{L^2(S_F)},\quad\forall F\in\Gamma_h\setminus\bigcup_{i=1}^N\Gamma_i$$

Combining the above estimates with Lemma 4.5 and Corollary 4.11 yields the bound (4.62) on R_Ω^2. For R_Λ^2, we have from Lemma 4.12 that

$$\begin{aligned}R_\Lambda^2=\sum_{i=0}^N h_\Lambda|A\,\mathrm{d}_s\hat{v}|^2_{s_i}\lesssim\sum_{i=0}^N\|\mathrm{d}_s(\hat{u}-\hat{v})\|^2_{L^2_A(\hat{S}_i)}+\sum_{i=0}^N h_\Lambda^2\sum_{\Lambda_\ell\subset\hat{S}_i}\|A\hat{f}+\mathrm{d}_s(A\,\mathrm{d}_s\hat{v})-PL_h\hat{v}\|^2_{L^2(\Lambda_\ell)}\\ +h_\Lambda^2\|\hat{L}_h(\hat{u}-\hat{v})\|^2_{L^2_P(\Lambda)}+h_\Lambda^2\|\overline{u}-\hat{u}\|^2_{L^2_P(\Lambda)}.\end{aligned}$$

Applying Corollary 4.11 and Lemma 4.5 yields the bound on R_Λ^2. ∎

5. Time dependent 3D-1D model. We now consider the time dependent model. For details on the derivation, well–posedness, and regularity properties of the system, we refer to [26]. The weak formulation of the time–dependent problem reads as follows. Find $\boldsymbol{u}=(u,\hat{u})\in\boldsymbol{V}=L^2(0,T;H^1_0(\Omega))\times L^2(0,T;H^1_A(\Lambda))$ with $(\partial_tu,\partial_t\hat{u})\in L^2(0,T;L^2(\Omega))\times L^2(0,T;L^2_A(\Lambda))$ such that

$$(\partial_tu,v)+(\partial_t(A\hat{u}),\hat{v})_\Lambda+\mathcal{A}(\boldsymbol{u},\boldsymbol{v})=(f,v)+(A\,\hat{f},\hat{v})_\Lambda,\quad\forall\boldsymbol{v}\in\boldsymbol{V}. \tag{5.1}$$

$$\boldsymbol{u}(0)=(u^0,\hat{u}^0)\in L^2(\Omega)\times L^2_A(\Lambda). \tag{5.2}$$

We recall that $\mathcal{A}$ is given in (2.15) and assume that $f\in L^2(0,T;L^2(\Omega))$ and $\hat{f}\in L^2(0,T;L^2_A(\Lambda))$ are given. We retain the assumptions on A and P from the previous sections, and we assume that they are independent of time. Consider a uniform partition of the time interval $[0,T]$ into N_T

sub-intervals with time step size τ. We use the notation $g^n(\cdot) = g(t^n, \cdot) = g(n\tau, \cdot)$ for any function g. Let $(u_h^0, \hat{u}_h^0) \in \mathbb{V}_h^\Omega \times \mathbb{V}_h^\Lambda$ be the L^2 projection of $(u^0, \hat{u}^0)$.

$$u_h^0 = \pi_h u^0, \quad \hat{u}_h^0 = \hat{\pi}_h \hat{u}^0.$$

A backward Euler dG approximation then reads as follows. Find $\boldsymbol{u}_h = (u_h^n, \hat{u}_h^n)_{1\le n\le N_T} \in \mathbb{V}_h^\Omega \times \mathbb{V}_h^\Lambda$ such that

$$\begin{aligned}(5.3)\quad \frac{1}{\tau}(u_h^n - u_h^{n-1}, v_h) + \frac{1}{\tau}(A(\hat{u}_h^n - \hat{u}_h^{n-1}), \hat{v}_h)_\Lambda + \mathcal{A}_h(\boldsymbol{u}_h^n, \boldsymbol{v}_h) \\ = (f^n, v_h) + (A\hat{f}^n, \hat{v}_h)_\Lambda, \quad \forall \boldsymbol{v}_h \in \mathbb{V}_h^\Omega \times \mathbb{V}_h^\Lambda.\end{aligned}$$

The form $\mathcal{A}_h$ is given in (3.15). To analyse the above scheme, we define the following elliptic projection: $\Pi_h(t) : H^1(0,T; H_0^1(\Omega)) \times H^1(0,T; H_A^1(\Lambda)) \to H^1(0,T; \mathbb{V}_h^\Omega) \times H^1(0,T; \mathbb{V}_h^\Lambda)$ such that for a given $\boldsymbol{g}(t) = (g(t), \hat{g}(t))$

$$\mathcal{A}_h(\Pi_h \boldsymbol{g}(t), \boldsymbol{v}_h) = (g(t), v_h)_\Omega + (A\,\hat{g}(t), \hat{v}_h)_\Lambda. \quad \forall \boldsymbol{v}_h \in \mathbb{V}_h^\Omega \times \mathbb{V}_h^\Lambda.$$

From the analysis of the previous section, for any $t > 0$, $\Pi_h \boldsymbol{g}(t)$ is well defined. Since $\mathcal{A}_h$ is linear and coercive and Π_h is continuous, $\partial_t(\Pi_h \boldsymbol{g}(t)) = \Pi_h \partial_t \boldsymbol{g}(t)$. Hereinafter, we assume that $(u, \hat{u}) \in H^1(0,T; H^{3/2-\eta}(\Omega)) \times H^1(0,T; H^2(\Lambda))$, $(\partial_{tt} u, \partial_{tt}(A\hat{u})) \in L^2(0,T; L^2(\Omega)) \times L^2(0,T; L^2(\Lambda))$, and $(f, \hat{f}) \in H^1(0,T; L^2(\Omega)) \times H^1(0,T; L^2(\Lambda))$. For smooth domains and for $(u^0, \hat{u}^0) \in H_0^1(\Omega) \times H^1(\Lambda)$, the $H^{3/2-\eta}$ spatial regularity on u is proven in [26, Proposition 4.2] and the H^2 spatial regularity for $\hat{u}$ can be expected since it solves a parabolic equation with an L^2–source term. By formally differentiating in time the parabolic 3D–1D problem and under sufficient assumptions on the initial conditions, the H^1 regularity in time for u and $\hat{u}$ can be expected, see for e.g [11, Chapter 7].

Now, for $\boldsymbol{u}(t) = (u(t), \hat{u}(t))$ and $\boldsymbol{f}(t) = (f(t), \hat{f}(t))$, we define the interpolant $\boldsymbol{\eta}_h(t) = (\eta_h(t), \hat{\eta}_h(t)) \in \mathbb{V}_h^\Omega \times \mathbb{V}_h^\Lambda$ such that

$$\boldsymbol{\eta}_h(t) = \Pi_h((f(t) - \partial_t u(t),\ A\hat{f}(t) - A\partial_t \hat{u}(t))).$$

Therefore, we have that

$$\mathcal{A}_h(\boldsymbol{\eta}_h(t), \boldsymbol{v}_h) = (f(t) - \partial_t u(t), v_h) + (A\,\hat{f}(t) - A\,\partial_t \hat{u}(t), \hat{v}_h)_\Lambda, \quad \forall \boldsymbol{v}_h \in \mathbb{V}_h^\Omega \times \mathbb{V}_h^\Lambda.$$

Since

$$\mathcal{A}(\boldsymbol{u}(t), \boldsymbol{v}) = (f(t) - \partial_t u(t), v) + (A\hat{f}(t) - A\partial_t \hat{u}(t), \hat{v})_\Lambda, \quad \forall \boldsymbol{v} \in H_0^1(\Omega) \times H_A^1(\Lambda),$$

we apply the error analysis of the previous section to obtain that for any $\eta > 0$

$$\begin{aligned}(5.4)\quad \|\boldsymbol{\eta}_h(t) - \boldsymbol{u}(t)\|_{\mathrm{DG}} \lesssim h^{1/2-\eta}(\|u(t)\|_{H^{3/2-\eta}(\Omega)} + \|\hat{u}(t)\|_{H_A^2(\Lambda)}) \\ + h(\|f(t) - \partial_t u(t)\|_{L^2(\Omega)} + \|\hat{f}(t) - \partial_t u(t)\|_{L_A^2(\Lambda)}).\end{aligned}$$

Here, for simplicity, we let $h_\Lambda \approx h$. It is also easy to see that

$$\begin{aligned}\partial_t \boldsymbol{\eta}_h(t) &= \partial_t \Pi_h((f(t) - \partial_t u(t),\ A\,\hat{f}(t) - A\,\partial_t \hat{u}(t))) \\ &= \Pi_h((\partial_t f(t) - \partial_{tt} u(t),\ A\,\partial_t \hat{f}(t) - A\,\partial_{tt} \hat{u}(t)).\end{aligned}$$

Therefore,

$$\mathcal{A}_h(\partial_t \boldsymbol{\eta}_h(t), \boldsymbol{v}_h) = (\partial_t f(t) - \partial_{tt} u(t), v_h) + (A\,\partial_t \hat{f}(t) - A\,\partial_{tt} \hat{u}(t), \hat{v}_h)_\Lambda, \quad \forall \boldsymbol{v}_h \in \mathbb{V}_h^\Omega \times \mathbb{V}_h^\Lambda.$$

Observing that

$$\mathcal{A}(\partial_t \boldsymbol{u}(t), \boldsymbol{v}) = (\partial_t f(t) - \partial_{tt} u(t), v) + (A\,\partial_t \hat{f}(t) - A\,\partial_{tt} \hat{u}(t), \hat{v})_\Lambda, \quad \forall \boldsymbol{v} \in H_0^1(\Omega) \times H_A^1(\Lambda),$$

we apply the previous analysis to obtain a bound on $\|\partial_t \boldsymbol{\eta}_h(t) - \partial_t \boldsymbol{u}(t)\|_{\mathrm{DG}}$ that is a similar to (5.4):

$$\|\partial_t \boldsymbol{\eta}_h(t) - \partial_t \boldsymbol{u}(t)\|_{\mathrm{DG}} \lesssim h^{1/2-\eta}(\|\partial_t u(t)\|_{H^{3/2-\eta}(\Omega)} + \|\partial_t \hat{u}(t)\|_{H^2_A(\Lambda)}) + h(\|\partial_t f(t) - \partial_{tt} u(t)\|_{L^2(\Omega)} + \|\partial_t \hat{f}(t) - \partial_{tt} u(t)\|_{L^2_A(\Lambda)}). \tag{5.5}$$

This interpolant allows us to prove the following result.

THEOREM 5.1. *For any $1 \le m \le N_T$, there holds*

$$\|u_h^m - u^m\|^2 + \|\hat{u}_h^m - \hat{u}^m\|^2_{L^2_A(\Lambda)} + \frac{C_{\mathrm{coerc}}}{4}\tau \sum_{n=1}^{m} \|\boldsymbol{u}_h^n - \boldsymbol{u}^n\|^2_{\mathrm{DG}} \lesssim \tau^2 + h^{1-2\eta}. \tag{5.6}$$

The above estimate holds under the assumptions: $(u, \hat{u}) \in H^1(0,T; H^{3/2-\eta}(\Omega)) \times H^1(0,T; H^2(\Lambda))$, $(\partial_{tt} u, \partial_{tt}(A\hat{u})) \in L^2(0,T; L^2(\Omega)) \times L^2(0,T; L^2(\Lambda))$, and $(f, \hat{f}) \in H^1(0,T; L^2(\Omega)) \times H^1(0,T; L^2(\Lambda))$.

Proof. We derive the error equation for $\boldsymbol{e}_h^n = (e_h^n, \hat{e}_h^n) = \boldsymbol{u}_h^n - \boldsymbol{\eta}_h^n$. For all $\boldsymbol{v}_h \in \mathbb{V}_h^\Omega \times \mathbb{V}_h^\Lambda$,

$$\frac{1}{\tau}(e_h^n - e_h^{n-1}, v_h) + \frac{1}{\tau}(A(\hat{e}_h^n - \hat{e}_h^{n-1}), \hat{v}_h)_\Lambda + \mathcal{A}_h(\boldsymbol{e}_h^n, \boldsymbol{v}_h) = \frac{1}{\tau}(\tau(\partial_t u)^n - (\eta_h^n - \eta_h^{n-1}), v_h) + \frac{1}{\tau}(\tau A(\partial_t \hat{u})^n - A(\hat{\eta}_h^n - \hat{\eta}_h^{n-1}), \hat{v}_h)_\Lambda. \tag{5.7}$$

The proof is based on energy arguments. We test (5.7) with $\boldsymbol{v}_h = \boldsymbol{e}_h^n$ and multiply by τ. With the coercivity property (3.16), we obtain

$$\frac{1}{2}(\|e_h^n\|^2 - \|e_h^{n-1}\|^2) + \frac{1}{2}(\|\hat{e}_h^n\|^2_{L^2_A(\Lambda)} - \|\hat{e}_h^{n-1}\|^2_{L^2_A(\Lambda)}) + \frac{C_{\mathrm{coerc}}}{2}\tau \|\boldsymbol{e}_h^n\|^2_{\mathrm{DG}} \lesssim (\tau(\partial_t u)^n - (\eta_h^n - \eta_h^{n-1}), e_h^n) + (A(\tau(\partial_t \hat{u})^n - (\hat{\eta}_h^n - \hat{\eta}_h^{n-1})), \hat{e}_h^n)_\Lambda = T_1 + T_2. \tag{5.8}$$

It is standard to show (with Cauchy-Schwarz's inequality, Taylor's theorem, and Poincaré's inequality (3.9)) that

$$T_1 \lesssim (\tau^{3/2}\|\partial_{tt} u\|_{L^2(t^{n-1}, t^n; L^2(\Omega))} + \tau^{1/2}\|\partial_t(u - \eta_h)\|_{L^2(t^{n-1}, t^n; L^2(\Omega))})\|e_h^n\|_{\mathbb{V}_h^\Omega}.$$

With Young's inequality, we then obtain

$$T_1 \le C\tau^2 \|\partial_{tt} u\|^2_{L^2(t^{n-1}, t^n; L^2(\Omega))} + C\|\partial_t(u - \eta_h)\|^2_{L^2(t^{n-1}, t^n; L^2(\Omega))} + \tau \frac{C_{\mathrm{coerc}}}{8}\|\boldsymbol{e}_h^n\|^2_{\mathrm{DG}}.$$

Similarly, we bound T_2 with

$$T_2 \le C\tau^2 \|A\partial_{tt} \hat{u}\|^2_{L^2(t^{n-1}, t^n; L^2(\Lambda))} + C\|A\partial_t(\hat{u} - \hat{\eta}_h)\|^2_{L^2(t^{n-1}, t^n; L^2(\Omega))} + \tau \frac{C_{\mathrm{coerc}}}{8}\|\boldsymbol{e}_h^n\|^2_{\mathrm{DG}}.$$

We use the above bounds in (5.8), and we sum the resulting bound over n. We obtain that

$$\|e_h^m\|^2 + \|\hat{e}_h^m\|^2_{L^2_A(\Lambda)} + \frac{C_{\mathrm{coerc}}}{4}\tau \sum_{n=1}^{m} \|\boldsymbol{e}_h^n\|^2_{\mathrm{DG}} \lesssim \tau^2(\|\partial_{tt} u\|^2_{L^2(0,T;L^2(\Omega))} + \|A\partial_{tt} \hat{u}\|^2_{0,T;L^2(\Omega))}) + \|\partial_t(u - \eta_h)\|^2_{L^2(0,T;L^2(\Omega))} + \|A\partial_t(\hat{u} - \hat{\eta}_h)\|^2_{L^2(0,T;L^2(\Omega))} + \|e_h^0\|^2 + \|\hat{e}_h^0\|^2_{L^2_A(\Lambda)}.$$

Then, the result follows by using the error estimates (5.4) and (5.5), approximation properties of the L^2 projections (4.4), and the triangle inequality. ∎

REMARK 1. *In the case of graded meshes, i.e. under the same mesh assumptions as Corollary 4.8, almost optimal spatial convergence rates in the dG norm hold. For example, for $k_1 = 1$, we have that for any $1 \le m \le N_T$,*

$$\|u_h^m - u^m\|^2 + \|\hat{u}_h^m - \hat{u}^m\|^2_{L^2_A(\Lambda)} + \frac{C_{\mathrm{coerc}}}{4}\tau \sum_{n=1}^{m} \|\boldsymbol{u}_h^n - \boldsymbol{u}^n\|^2_{\mathrm{DG}} \lesssim \tau^2 + h^{2(1-2\eta)}. \tag{5.9}$$

The above estimate holds under the additional assumption that $u \in H^1(0,T;H^2(\Omega\backslash\overline{B}_\Lambda)\cap H^2(B_\Lambda))$. *The proof follows from the same argument as before where similar estimates to* (4.32) *are used for the dG norm of* $\boldsymbol{\eta}_h - \boldsymbol{u}$ *and of* $\partial_t(\boldsymbol{\eta}_h - \boldsymbol{u})$. *For* $k_1 > 1$, *one can also derive almost optimal rates under additional regularity requirements on the solution. We omit the details for brevity.*

6. Extension to 1D networks embedded in a 3D domain. We extend the above numerical method and model to a 1D network in a 3D domain. We adopt the notation of [9] where a hybridized dG method is used for convection diffusion problems in a network. Here, we only introduce Lagrange multipliers on the bifurcation nodes, and we couple the network model to the 3D equations. We do not analyze this dG method for the 3D-1D network model beyond showing well–posedness and local mass conservation at bifurcation points. The error analysis will be the object of future work.

A network is represented by a finite, directed, and connected oriented graph $\mathcal{G}(\mathcal{V},\mathcal{E})$ where $\mathcal{V}$ is the set of vertices and $\mathcal{E}$ is the set of edges. We let $\mathcal{E}(\mathsf{v})$ denote the set of edges sharing a vertex v. The boundary of the graph is then defined by $\mathcal{V}_\partial = \{\mathsf{v}\in\mathcal{V},\ \mathrm{card}(\mathcal{E}(\mathsf{v}))=1\}$. For a given edge $\mathsf{e} = (\mathsf{v}^{\mathsf{e}}_{\mathrm{in}}, \mathsf{v}^{\mathsf{e}}_{\mathrm{out}})$, we define the function $n_{\mathsf{e}} : \mathcal{V}\to\{-1,0,1\}$ with

$$n_{\mathsf{e}}(\mathsf{v}^{\mathsf{e}}_{\mathrm{in}}) = 1,\ n_{\mathsf{e}}(\mathsf{v}^{\mathsf{e}}_{\mathrm{out}}) = -1 \text{ and } n_{\mathsf{e}}(\mathsf{v}) = 0, \quad \forall \mathsf{v}\in\mathcal{V}\setminus\{\mathsf{v}^{\mathsf{e}}_{\mathrm{in}}, \mathsf{v}^{\mathsf{e}}_{\mathrm{out}}\}.$$

The collection of bifurcation points is denoted by $\mathcal{B} = \{\mathsf{v}\in\mathcal{V},\ \mathrm{card}(\mathcal{E}(\mathsf{v}))\geq 3\}$. For each $\mathsf{e}\in\mathcal{E}$, we define a surrounding cylinder B_{e} of cross–section Θ_{e} with area A_{e} and perimeter P_{e}. The L^2_P space over the graph is defined by

$$L^2_P(\mathcal{G}) = \{u :\ u_{\mathsf{e}} = u|_{\mathsf{e}} \in L^2_{P_{\mathsf{e}}}(\mathsf{e}),\ \forall \mathsf{e}\in\mathcal{E}\}. \tag{6.1}$$

This 1D-network is embedded in a 3D domain Ω. The surrounding cylinders B_{e} are all strictly included in Ω. In Ω, we solve for u satisfying (in the distributional sense)

$$-\Delta u + \xi(\overline{u}-\hat{u})\delta_{\mathcal{G}} = f \quad \text{in } \Omega, \quad u = 0 \text{ on } \partial\Omega, \tag{6.2}$$

and for each $\mathsf{e}\in\mathcal{E}$, we solve for a 1D solution $\hat{u}_{\mathsf{e}}$ satisfying

$$-\mathrm{d}_s(A_{\mathsf{e}}\,\mathrm{d}_s\hat{u}_{\mathsf{e}}) + P_{\mathsf{e}}(\hat{u}_{\mathsf{e}} - \overline{u}_{\mathsf{e}}) = \hat{f}_{\mathsf{e}} \text{ in } \mathsf{e}. \tag{6.3}$$

The coefficient ξ is a piecewise positive constant on each edge of the graph. The function $\overline{u}$ is defined by

$$\overline{u}|_{\mathsf{e}} = \overline{u}_{\mathsf{e}} = \frac{1}{P_{\mathsf{e}}}\int_{\partial\Theta_{\mathsf{e}}} u, \quad \forall \mathsf{e}\in\mathcal{E}.$$

The functional $\xi(\overline{u}-\hat{u})\delta_{\mathcal{G}}$ is defined by

$$\xi(\overline{u}-\hat{u})\delta_{\mathcal{G}}(v) = \sum_{\mathsf{e}\in\mathcal{E}}\int_{\mathsf{e}} \xi_{\mathsf{e}}\,P_{\mathsf{e}}(\overline{u}_{\mathsf{e}} - \hat{u}_{\mathsf{e}})\overline{v}_{\mathsf{e}}, \quad \forall v\in H^1(\Omega).$$

We supplement the above system with the following boundary conditions which impose conservation of fluxes and continuity at bifurcation points. On the boundary, we impose homogeneous Neumann conditions.

$$\sum_{\mathsf{e}\in\mathcal{E}(\mathsf{v})} A_{\mathsf{e}}\,\mathrm{d}_s\hat{u}_{\mathsf{e}}(\mathsf{v})n_{\mathsf{e}}(\mathsf{v}) = 0 \text{ and } \hat{u}_{\mathsf{e}}(\mathsf{v}) = \hat{u}_{\mathsf{e}'}(\mathsf{v}), \qquad \forall \mathsf{v}\in\mathcal{B},\ \forall \mathsf{e},\mathsf{e}'\in\mathcal{E}(\mathsf{v}), \tag{6.4}$$

$$A_{\mathsf{e}}\,\mathrm{d}_s\hat{u}_{\mathsf{e}}(\mathsf{v}) = 0, \qquad \forall \mathsf{v}\in\mathcal{V}_\partial,\ \mathsf{e}\in\mathcal{E}(\mathsf{v}). \tag{6.5}$$

To summarise, the 3D-1D network model consists of (6.2)-(6.3) with boundary conditions (6.4)-(6.5). The above model can also be found in [22, Section 2.5]. We now introduce a dG formulation for this model.

6.1. DG for the 3D-1D network model. For each $\mathsf{e} \in \mathcal{E}$, we denote by h_e the characteristic length of a partition of the edge e and we introduce a mesh and a space $\mathbb{V}_h^\mathsf{e}$ of degree k_e similar to (3.2). Then, we define the broken polynomial space

$$\mathbb{V}_h^\mathcal{G} = \{\hat{v}_h : \ \hat{v}_h|_\mathsf{e} = \hat{v}_{\mathsf{e},h} \in \mathbb{V}_h^\mathsf{e}\}.$$

We will use a hybridization technique to handle the values of the discrete solution at the bifurcation points. Thus, we define

$$\mathbb{V}_h^\mathcal{B} = \{\tilde{w}_h = (\tilde{w}_{\mathsf{v},h})_{\mathsf{v}\in\mathcal{B}}, \ \sum_{\mathsf{v}\in\mathcal{B}} \tilde{w}_{\mathsf{v},h}^2 < \infty\}. \tag{6.6}$$

We now define the form $b_\mathsf{v} : (\mathbb{V}_h^\Omega \times \mathbb{V}_h^\mathcal{G} \times \mathbb{V}_h^\mathcal{B})^2 \to \mathbb{R}$ which enforces conditions at the bifurcation points, see Remark 2. For $\mathsf{v} \in \mathcal{B}$, define

$$\begin{aligned} b_\mathsf{v}((u_h,\hat{u}_h,\tilde{u}_h),(w_h,\hat{w}_h,\tilde{w}_h)) &= \sum_{\mathsf{e}\in\mathcal{E}(\mathsf{v})} A_\mathsf{e}\, \mathrm{d}_s\hat{u}_{\mathsf{e},h}(\mathsf{v}) n_\mathsf{e}(\mathsf{v})\,(\hat{w}_{\mathsf{e},h}(\mathsf{v}) - \tilde{w}_{\mathsf{v},h}) \\ &+ \sum_{\mathsf{e}\in\mathcal{E}(\mathsf{v})} A_\mathsf{e}\, \mathrm{d}_s\hat{w}_{\mathsf{e},h}(\mathsf{v}) n_\mathsf{e}(\mathsf{v})\,(\hat{u}_{\mathsf{e},h}(\mathsf{v}) - \tilde{u}_{\mathsf{v},h}) + \sum_{\mathsf{e}\in\mathcal{E}(\mathsf{v})} \frac{\sigma_\mathsf{v}}{h_\mathsf{e}}(\hat{u}_{\mathsf{e},h}(\mathsf{v}) - \tilde{u}_{\mathsf{v},h})\,(\hat{w}_{\mathsf{e},h}(\mathsf{v}) - \tilde{w}_{\mathsf{v},h}). \end{aligned} \tag{6.7}$$

The full dG formulation reads as follows. Find $(u_h,\hat{u}_h,\tilde{u}_h) \in \mathbb{V}_h^\Omega \times \mathbb{V}_h^\mathcal{G} \times \mathbb{V}_h^\mathcal{B}$ such that for all $(w_h,\hat{w}_h,\tilde{w}_h) \in \mathbb{V}_h^\Omega \times \mathbb{V}_h^\mathcal{G} \times \mathbb{V}_h^\mathcal{B}$, there holds

$$a_h(u_h,w_h) + \sum_{\mathsf{e}\in\mathcal{E}} b_\mathsf{e}(\overline{u}_{\mathsf{e},h} - \hat{u}_{\mathsf{e},h}, \overline{w}_{\mathsf{e},h}) = (f,w_h), \tag{6.8}$$

$$\begin{aligned} \sum_{\mathsf{e}\in\mathcal{E}} a_{\mathsf{e},h}(\hat{u}_{\mathsf{e},h},\hat{w}_{\mathsf{e},h}) + \sum_{\mathsf{e}\in\mathcal{E}} b_\mathsf{e}(\hat{u}_{\mathsf{e},h} - \overline{u}_{\mathsf{e},h}, \hat{w}_{\mathsf{e},h}) \\ + \sum_{\mathsf{v}\in\mathcal{B}} b_\mathsf{v}((u_h,\hat{u}_h,\tilde{u}_h),(w_h,\hat{w}_h,\tilde{w}_h)) = \sum_{\mathsf{e}\in\mathcal{E}} (\hat{f}_\mathsf{e},\hat{w}_{\mathsf{e},h})_{L^2_{A_\mathsf{e}}(\mathsf{e})}. \end{aligned} \tag{6.9}$$

In the scheme above, the form a_h is the same one defined by (3.12) and the forms $a_{\mathsf{e},h}$ and b_e correspond to the forms $a_{\Lambda,h}$ and b_Λ with $\Lambda = \mathsf{e}$. For instance, we write

$$b_\mathsf{e}(\hat{v},\hat{w}) = (\xi_\mathsf{e}\hat{v},\hat{w})_{L^2_{P_\mathsf{e}}(\mathsf{e})}, \quad \forall \hat{v},\hat{w} \in L^2_{P_\mathsf{e}}(\mathsf{e}).$$

Remark 2 (Bifurcation conditions). *For a given $\mathsf{v} \in \mathcal{B}$, let $\tilde{w}_h \in \mathbb{V}_h^\mathcal{B}$ be such that $\tilde{w}_{\mathsf{v},h} = 1$ and zero otherwise. Choosing $(w_h,\hat{w}_h,\tilde{w}_h) = (0,0,\tilde{w}_h)$ in (6.9) yields:*

$$\sum_{\mathsf{e}\in\mathcal{E}(\mathsf{v})} A_\mathsf{e}\, \mathrm{d}_s\hat{u}_{\mathsf{e},h}(\mathsf{v}) n_\mathsf{e}(\mathsf{v}) + \sum_{\mathsf{e}\in\mathcal{E}(\mathsf{v})} \frac{\sigma_\mathsf{v}}{h_\mathsf{e}}(\hat{u}_{\mathsf{e},h}(\mathsf{v}) - \tilde{u}_{\mathsf{v},h}) = 0, \quad \forall \mathsf{v} \in \mathcal{B}. \tag{6.10}$$

That is, up to jump terms, the discrete dG scheme locally conserves the fluxes, see (6.4), at each bifurcation point.

Lemma 6.1 (Well–posedness). *There exists a unique solution for the problem given in (6.8) and (6.9).*

Proof. For any $(u_h,\hat{u}_h,\tilde{u}_h) \in \mathbb{V}_h^\Omega \times \mathbb{V}_h^\mathcal{G} \times \mathbb{V}_h^\mathcal{B}$, let

$$\begin{aligned} \mathcal{X} = a_h(u_h,u_h) + \sum_{\mathsf{e}\in\mathcal{E}} a_{\mathsf{e},h}(\hat{u}_{\mathsf{e},h},\hat{u}_{\mathsf{e},h}) \\ + \sum_{e\in\mathcal{E}} b_\mathsf{e}(\overline{u}_{\mathsf{e},h} - \hat{u}_{\mathsf{e},h}, \overline{u}_{\mathsf{e},h} - \hat{u}_{\mathsf{e},h}) + \sum_{\mathsf{v}\in\mathcal{B}} b_\mathsf{v}((u_h,\hat{u}_h,\tilde{u}_h),(u_h,\hat{u}_h,\tilde{u}_h)). \end{aligned}$$

It suffices to show that

$$\mathcal{X} \gtrsim \|u_h\|^2_{\mathbb{V}_h^\Omega} + \sum_{\mathsf{e}\in\mathcal{E}} (|\hat{u}_h|^2_{\mathbb{V}_h^\mathsf{e}} + \|\overline{u}_{\mathsf{e},h} - \hat{u}_{e,h}\|^2_{L^2_P(\mathsf{e})}) + \sum_{\mathsf{v}\in\mathcal{B}} \sum_{\mathsf{e}\in\mathcal{E}(\mathsf{v})} \frac{\sigma_\mathsf{e}}{h_\mathsf{e}} (\hat{u}_{\mathsf{e},h}(\mathsf{v}) - \tilde{u}_{\mathsf{v},h})^2, \tag{6.11}$$

since the right hand side above defines a norm. Here, $|\cdot|_{\mathbb{V}_h^\mathsf{e}}$ is defined in the same way as (3.10). Consider the last term in $\mathcal{X}$ and recall the trace estimate:

$$|\mathrm{d}_s \hat{u}_{\mathsf{e},h}(\mathsf{v}) \cdot \boldsymbol{n}_\mathsf{e}(\mathsf{v})| \le C_{\mathrm{tr}} h_\mathsf{e}^{-1/2} \|\mathrm{d}_s \hat{u}_{\mathsf{e},h}\|_{L^2(\mathsf{e}_\mathsf{v})}, \tag{6.12}$$

where e_v is the mesh element of e incident to v. Then, with the above estimate, Cauchy–Schwarz's inequality for sums applied twice, and Young's inequality, we bound the first term in $\sum_{\mathsf{v}\in\mathcal{B}} b_\mathsf{v}((u_h,\hat{u}_h,\tilde{u}_h),(u_h,\hat{u}_h,\tilde{u}_h))$ by

$$\sum_{\mathsf{v}\in\mathcal{B}} \sum_{\mathsf{e}\in\mathcal{E}(\mathsf{v})} |A_\mathsf{e}\, \mathrm{d}_s \hat{u}_{\mathsf{e},h}(\mathsf{v}) n_\mathsf{e}(\mathsf{v}) \, (\hat{u}_{\mathsf{e},h}(\mathsf{v}) - \tilde{u}_{\mathsf{v},h})| \le \frac{1}{2} \sum_{\mathsf{v}\in\mathcal{B}} \sum_{\mathsf{e}\in\mathcal{E}(\mathsf{v})} C_\mathsf{e} |\hat{u}_h|^2_{\mathcal{T}_\mathsf{e}^h} + \sum_{\mathsf{v}\in\mathcal{B}} \sum_{\mathsf{e}\in\mathcal{E}(\mathsf{v})} \frac{C_3}{h_\mathsf{e}} (\hat{u}_{\mathsf{e},h}(\mathsf{v}) - \tilde{u}_{\mathsf{v},h})^2,$$

where C_e is the coercivity constant of $a_{\mathsf{e},h}$, similar to (3.17), and $C_3 > 0$ is a positive constant depending on C_e, on C_{tr} and on A_e. Thus, if σ_v is large enough, there exists a constant $C_4 > 0$ such that

$$\sum_{\mathsf{v}\in\mathcal{B}} b_\mathsf{v}((u_h,\hat{u}_h,\tilde{u}_h),(u_h,\hat{u}_h,\tilde{u}_h)) + \frac{1}{2} \sum_{\mathsf{e}\in\mathcal{E}} C_\mathsf{e} |\hat{u}_h|^2_{\mathcal{T}_\mathsf{e}^h} \ge \sum_{\mathsf{v}\in\mathcal{B}} \sum_{\mathsf{e}\in\mathcal{E}(\mathsf{v})} \frac{C_4}{h_\mathsf{e}} (\hat{u}_{\mathsf{e},h}(\mathsf{v}) - \tilde{u}_{\mathsf{v},h})^2,$$

It then follows that

$$\sum_{\mathsf{e}\in\mathcal{E}} a_{\mathsf{e},h}(\hat{u}_{\mathsf{e},h},\hat{u}_{\mathsf{e},h}) + \sum_{\mathsf{v}\in\mathcal{B}} b_\mathsf{v}(u_h,\hat{u}_h,\tilde{u}_h),(u_h,\hat{u}_h,\tilde{u}_h)) \ge \frac{1}{2} \sum_{\mathsf{e}\in\mathcal{E}} C_\mathsf{e} |\hat{u}_h|^2_{\mathcal{T}_\mathsf{e}^h} + \sum_{\mathsf{v}\in\mathcal{B}} \sum_{\mathsf{e}\in\mathcal{E}(\mathsf{v})} \frac{C_4}{h_\mathsf{e}} (\hat{u}_{\mathsf{e},h}(\mathsf{v}) - \tilde{u}_{\mathsf{v},h})^2.$$

From here, we use the coercivity results (3.17) and the definition of b_e to conclude that (6.11) holds. We omit the details for brevity. ∎

7. Numerical results. We present results for manufactured solutions in a 3D–1D setting and in a 1D vessel network. We also show results for a realistic 1D network in a 3D domain.

7.1. Manufactured solutions with one vessel in a 3D domain. In this first example, we consider manufactured solutions and compute error rates. Let $\Omega = (-0.5, 0.5)^3$ contain $\Lambda = \{(0,0,z), z \in (-0.5, 0.5)\}$ with a surrounding cylinder of constant radius $R = 0.05$. Denoting by r the distance to the line Λ, the exact solutions are

$$u = \begin{cases} \frac{\xi}{\xi+1}(1 - R\ln(\frac{r}{R}))\hat{u}, & r > R, \\ \frac{\xi}{\xi+1}\hat{u}, & r \le R. \end{cases} \quad \text{and} \quad \hat{u} = \sin(\pi z) + 2. \tag{7.1}$$

The above 3D solution is obtained from the observation that [10, eq. 40], see also [19]:

$$\int_\Omega -(\partial_{xx}\, u + \partial_{yy} u)\; v = \int_\Gamma \frac{\xi}{\xi+1} \hat{u}\, v = -\int_\Lambda \xi\, P\, (\overline{u} - \hat{u})\overline{v}. \tag{7.2}$$

We set $\xi = 1$, and we modify the source terms $f, \hat{f}$ and the boundary conditions so that the equations are satisfied. The parameters are set to $\epsilon_1 = \epsilon_2 = -1$, $k_1 = k_2 = 1$, and $\sigma_\Omega = \sigma_\Lambda = 30$. For all our examples, we use the FEniCS finite element framework [1, 23] and the $(\text{FEniCS})_{ii}$

module [20]. We compute the solution $(u_h, \hat{u}_h)$, the L^2 and the H^1 norms of the errors $e_h = u - u_h$ and $\hat{e}_h = \hat{u} - \hat{u}_h$ on a family of uniform meshes created by by FEniCS "BoxMesh" with $6N^3$ number of elements. The results reported in Table 7.1 corroborate the error estimates established in Corollary 4.7. In particular, we observe that $\|e_h\|_{H^1(\Omega)}$ converges at a rate slightly higher than 0.5 while for $\|\hat{e}_h\|_{H^1(\Lambda)}$ linear convergence can be seen. In the L^2–norms we observe improved error rates. Due to the coupling and the low regularity of the 3D solution, it is not clear whether one can prove improved optimal error rates of $3/2 - \eta$ and of 2 for the 3D and 1D solutions respectively.

N	$\|e_h\|_{H^1(\Omega)}$	rate	$\|e_h\|_{L^2(\Omega)}$	rate	$\|\hat{e}_h\|_{H^1(\Lambda)}$	rate	$\|\hat{e}_h\|_{L^2(\Lambda)}$	rate
4	2.313e-01	-	1.562e-02	-	5.008e-01	-	3.663e-02	-
8	1.300e-01	0.832	4.714e-03	1.729	2.519e-01	0.992	1.779e-02	1.042
16	8.323e-02	0.643	1.457e-03	1.694	1.262e-01	0.998	7.832e-03	1.184
32	5.247e-02	0.666	4.345e-04	1.746	6.308e-02	1.000	3.374e-03	1.215
64	3.292e-02	0.673	1.171e-04	1.891	3.150e-02	1.002	8.293e-04	2.024

TABLE 7.1

L^2 and H^1 norms of the errors $(e_h, \hat{e}_h)$ and rates between the 3D-1D exact solution (7.1) and the computed solutions on a family of uniform meshes.

7.2. Manufactured solution for a vessel network. Next, we verify the convergence of the dG scheme for the 1D network model. Precisely, in this example, we now consider only the Poisson problem posed on the network $-\Delta\hat{u} = \hat{f}$ on $\mathcal{G}$ complemented with (6.4) and homogeneous Dirichlet conditions on $\mathcal{V}_\partial$, and we do not solve for a 3D solution. The dG scheme for this 1D diffusion problem problem is given in (6.9) with $u_h = v_h = \xi = 0$ and the penalty parameters set as $\sigma_{\mathsf{e}} = \sigma_{\mathsf{v}} = 10$. We consider the network embedded in $\mathbb{R}^2$ shown in Table 7.2 which includes 3 bifurcations, i.e. $|\mathcal{B}| = 3$, located at $\mathsf{v}_1 = (0,1)$, $\mathsf{v}_2 = (-1,2)$, $\mathsf{v}_3 = (1,2)$ while the remaining nodes are placed at $\mathsf{v}_0 = (0,0)$, $\mathsf{v}_4 = (-1.5,3)$, $\mathsf{v}_5 = (-0.5,3)$, $\mathsf{v}_6 = (0.5,3)$, $\mathsf{v}_7 = (1.5,3)$. Given $\mathcal{G}$, we consider the following solution and data

$$\hat{u} = \begin{cases} y + \cos 2\pi y, & (x,y) \in \mathsf{e}_0 \\ 2 + \frac{1}{2}\sqrt{2}(y-1), & (x,y) \in \mathsf{e}_{1\le i\le 2} \\ 2 + \frac{1}{2}\sqrt{2} + \frac{1}{8}\sqrt{5}(y-2), & (x,y) \in \mathsf{e}_{3\le i\le 6} \end{cases}, \quad \hat{f} = \begin{cases} 4\pi^2 \cos 2\pi y, & (x,y) \in \mathsf{e}_0 \\ 0, & (x,y) \in \mathsf{e}_{i\neq 0} \end{cases}. \tag{7.3}$$

Using (7.3) and the dG scheme with linear polynomials we consider approximation properties of the method with respect to the norm

$$\|(\hat{e}_h, \tilde{e}_h)\|^2_{\mathbb{V}_h^{\mathcal{G}} \times \mathbb{V}_h^{\mathcal{B}}} = \sum_{\mathsf{e}\in\mathcal{E}} \|\hat{e}_h\|^2_{\mathbb{V}_{\mathsf{e}}^h} + \sum_{\mathsf{v}\in\mathcal{B}} \sum_{\mathsf{e}\in\mathcal{E}(\mathsf{v})} \frac{\sigma_{\mathsf{e}}}{h_{\mathsf{e}}} (\hat{u}_{\mathsf{e},h}(v) - \tilde{u}_{\mathsf{v},h})^2, \tag{7.4}$$

where $\|\hat{e}_h\|^2_{\mathbb{V}_{\mathsf{e}}^h}$ is a slight modification to (3.10) to also include boundary terms. Table 7.2 reports the errors in the norm given in (7.4). From numerical analysis of interior penalty and of hybridizable dG methods, we expect first order convergence in the norm given above. This is what we observe in Table 7.2. Further, we compute the term $j_h(\mathsf{v}) = \sum_{\mathsf{e}\in\mathcal{E}(\mathsf{v})} \mathrm{d}_s \hat{u}_{\mathsf{e},h}(\mathsf{v}) n_{\mathsf{e}}(\mathsf{v})$ accounting for conservation of mass. Considering Remark 2, we expect this term to converge at a similar rate to the norm given in (7.4). This is indeed what we observe.

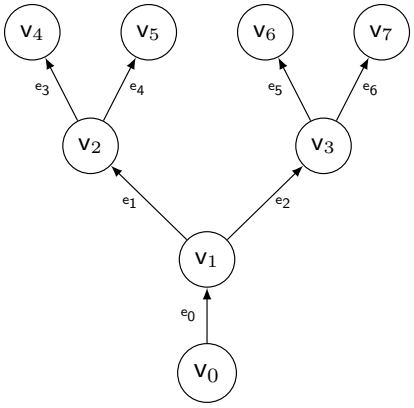

h	$\|(\hat{e}_h, \tilde{e}_h)\|_{\mathbb{V}_h^{\mathcal{G}} \times \mathbb{V}_h^{\mathcal{B}}}$	rate	$\max_{\mathsf{v}\in\mathcal{B}} \|j_h(\mathsf{v})\|$	rate
5.00e-1	1.420	–	1.242	–
2.50e-1	9.705e-1	5.49	4.683e-1	1.41
1.25e-1	4.268e-1	1.19	1.759e-1	1.41
6.25e-2	1.809e-1	1.24	7.807e-2	1.17
3.13e-2	7.896e-2	1.18	3.770e-2	1.05
1.56e-2	3.698e-2	1.11	1.868e-2	1.01
7.81e-3	1.771e-2	1.06	9.320e-3	1.00
3.91e-3	8.656e-3	1.03	4.657e-3	1.00
1.95e-3	4.277e-3	1.02	2.328e-3	1.00
9.77e-4	2.126e-3	1.01	1.164e-3	1.00
4.88e-4	1.060e-3	1.00	5.821e-4	1.00
2.44e-4	5.291e-4	1.00	2.910e-4	1.00

TABLE 7.2

Error convergence and flux conservation of the DG scheme defined as part of (6.8)-(6.9) and applied to the standalone diffusion problem on the network shown to the left. Here $\hat{e}_h = u - \hat{u}_h$, $\tilde{e}_h = u - \tilde{u}_h$ with u the exact solution (7.3). The norm is defined in (7.4). Following Remark 2, we let $j_h(\mathsf{v}) = \sum_{\mathsf{e}\in\mathcal{E}(\mathsf{v})} \mathrm{d}_s \hat{u}_{\mathsf{e},h}(\mathsf{v}) n_{\mathsf{e}}(\mathsf{v})$. We set the polynomial degree $k_{\mathsf{e}} = 1$.

7.3. Coupled 3D-1D simulation in realistic networks. In Figure 7.1, we finally illustrate the capabilities of our dG scheme to model tissue micro-circulation in a realistic setting. To this end, we utilize the data set [15] which includes vasculature of a $1\,\mathrm{mm}^3$ of a mouse cortex, and we let $\mathcal{G}$ be defined in terms of arteries and venules of this network, leaving out the capillaries. The vessel radius in the network ranges approximately from $5\,\mu$m to $35\,\mu$m. The 3D domain Ω is then defined as a bounding box of $\mathcal{G}$ of dimensions $[570.8, 518.7, 992.0]\,\mu$m. Upon discretization (with a uniform structured mesh, $h \approx 57.3\,\mu$m and $h_\Lambda \approx 0.9\,\mu$m), $\dim\mathbb{V}_h^\Omega = 196608$, $\dim\mathbb{V}_h^{\mathcal{G}} = 11196$, and $\dim\mathbb{V}_h^{\mathcal{B}} = 57$.

In (2.6), we then apply homogeneous Dirichlet and Neumann conditions on u and $\hat{u}$ respectively and, for simplicity, set $\xi = 1$ and $f = 0$, $\hat{f} = 1$. The obtained solution fields are shown in Figure 7.1; as a result of the coupling, the concentration u is higher in the vicinity of the network than elsewhere in the 3D domain.

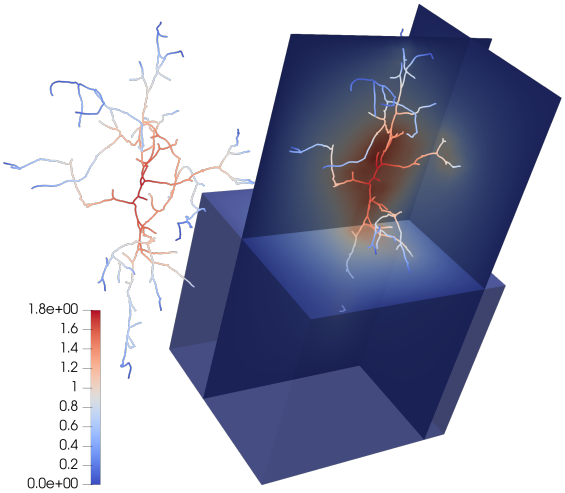

FIG. 7.1. *Numerical solutions $\hat{u}_h$ and u_h due to the dG scheme (6.8)-(6.9) applied to the coupled 3D-1D problem (6.2)–(6.3) with bifurcation conditions (6.4) considered on a realistic network taken from [15].*

REMARK 3. *While dG methods offer advantages over their continuous counterparts, it is well known that the number of degrees of freedom (DOFs) for dG methods is higher than that of continuous finite element methods (cG). See Table 7.3 for a comparison with respect to DOFs and*

scheme	$n_{\text{dofs}}\Omega$	$n_{\text{dofs}}\Lambda$	$t_{\text{asmbl}}a_h$ [s]	$t_{\text{solve}}a_h$ [s]	$t_{\text{asmbl}}\mathcal{A}_h$ [s]	$t_{\text{solve}}\mathcal{A}_h$ [s]
dG	196608	11253	0.25	19.4 (50)	11.1	52.0 (50)
cG	9537	5598	0.025	0.03 (8)	6.6	0.19 (16)

TABLE 7.3

Cost comparison of discretizations of the coupled 3D-1D problem (6.2)–(6.3) using the realistic network from [15] (leaving out the capillaries) and the mesh size of the example above. The dG scheme (6.8)-(6.9) with $k_1 = k_2 = 1$ is compared with the continuous linear Lagrange elements discretization [22, 26] in terms of (i) dimensionality of the approximation spaces, (ii) assembly and solution times of the Poisson problem induced by the bilinear form a_h (3.12) and (iii) assembly and solution times of the coupled problem, see (6.8)-(6.9). The systems are solved by preconditioned conjugate gradient method with (identical) algebraic multigrid preconditioner. Numbers in the brackets show the number of Krylov iterations to convergence (same convergence criteria are used in all the cases).

assembly and solution time for the coupled 3D–1D network problem of this section. It is observed that the increase in the DOFs is primarily caused by the 3D–discretization and not by the hybrid dG method of the 1D network. Further, we remark that the advantages of dG methods, such as local mass conservation and stability, are particularly apparent for transient advection–dominated diffusion problems. Here, we focus on the analysis of the elliptic case. We believe this to be a necessary first step to study dG approximations of 3D-1D advection diffusion systems where we expect to need the elliptic projection for the error analysis. This setting along with a computational study on the balance between accuracy and cost is an interesting future research direction.

8. Conclusions. Interior penalty discontinuous Galerkin methods are introduced for coupled 3D-1D problems. These models span several areas of applications such as modeling flow and transport in vascularized tissue. We analyze dG approximations for the steady state problem and a backward Euler dG method for the time dependent problem. Our analysis is valid under minimal assumptions on the regularity of the solution and on the mesh. Recovering almost optimal rates for graded meshes is also shown, under sufficient regularity assumptions. Further, we propose a novel dG method with hybridization for a network of vessels in a 3D surrounding. The method, up to jump terms, locally conserves mass at bifurcation points. Numerical results demonstrate our error analysis.

REFERENCES

[1] Martin Alnæs, Jan Blechta, Johan Hake, August Johansson, Benjamin Kehlet, Anders Logg, Chris Richardson, Johannes Ring, Marie E Rognes, and Garth N Wells. The FEniCS project version 1.5. *Archive of Numerical Software*, 3(100), 2015.

[2] Thomas Apel, Anna-Margarete Sändig, and John R Whiteman. Graded mesh refinement and error estimates for finite element solutions of elliptic boundary value problems in non-smooth domains. *Mathematical Methods in the Applied Sciences*, 19(1):63–85, 1996.

[3] Laura Cattaneo and Paolo Zunino. A computational model of drug delivery through microcirculation to compare different tumor treatments. *International Journal for Numerical Methods in Biomedical Engineering*, 30(11):1347–1371, 2014.

[4] Carlo D'Angelo. Multiscale modelling of metabolism and transport phenomena in living tissues. Technical report, EPFL, 2007.

[5] Carlo D'Angelo. Finite element approximation of elliptic problems with Dirac measure terms in weighted spaces: applications to one-and three-dimensional coupled problems. *SIAM Journal on Numerical Analysis*, 50(1):194–215, 2012.

[6] Carlo D'angelo and Alfio Quarteroni. On the coupling of 1D and 3D diffusion-reaction equations: application to tissue perfusion problems. *Mathematical Models and Methods in Applied Sciences*, 18(08):1481–1504, 2008.

[7] Daniele Antonio Di Pietro and Alexandre Ern. *Mathematical Aspects of Discontinuous Galerkin Methods*, volume 69. Springer Science & Business Media, 2011.

[8] Irene Drelichman, Ricardo G Durán, and Ignacio Ojea. A weighted setting for the numerical approximation of the Poisson problem with singular sources. *SIAM Journal on Numerical Analysis*, 58(1):590–606, 2020.

[9] Herbert Egger and Nora Philippi. A hybrid-dG method for singularly perturbed convection-diffusion equations on pipe networks. *ESAIM: Mathematical Modelling and Numerical Analysis*, 57(4):2077–2095, 2023.

[10] Björn Engquist, Anna-Karin Tornberg, and Richard Tsai. Discretization of Dirac delta functions in level set methods. *Journal of Computational Physics*, 207(1):28–51, 2005.

[11] Lawrence C Evans. *Partial Differential Equations*, volume 19. American Mathematical Society, 2010.

[12] Vivette Girault, Jizhou Li, and Beatrice Rivière. Strong convergence of discrete DG solutions of the heat equation. *Journal of Numerical Mathematics*, 24(4):235–252, 2016.
[13] Ingeborg G Gjerde, Kundan Kumar, and Jan M Nordbotten. A singularity removal method for coupled 1D–3D flow models. *Computational Geosciences*, 24(2):443–457, 2020.
[14] Ingeborg G Gjerde, Kundan Kumar, and Jan M Nordbotten. A mixed approach to the Poisson problem with line sources. *SIAM Journal on Numerical Analysis*, 59(2):1117–1139, 2021.
[15] Florian Goirand, Tanguy Le Borgne, and Sylvie Lorthois. Network-driven anomalous transport is a fundamental component of brain microvascular dysfunction. *Nature Communications*, 12(1):7295, 2021.
[16] Thirupathi Gudi. A new error analysis for discontinuous finite element methods for linear elliptic problems. *Mathematics of Computation*, 79(272):2169–2189, 2010.
[17] Ohannes A Karakashian and Frederic Pascal. A posteriori error estimates for a discontinuous Galerkin approximation of second-order elliptic problems. *SIAM Journal on Numerical Analysis*, 41(6):2374–2399, 2003.
[18] T Köppl and Barbara Wohlmuth. Optimal a priori error estimates for an elliptic problem with Dirac right-hand side. *SIAM Journal on Numerical Analysis*, 52(4):1753–1769, 2014.
[19] Tobias Köppl, Ettore Vidotto, Barbara Wohlmuth, and Paolo Zunino. Mathematical modeling, analysis and numerical approximation of second-order elliptic problems with inclusions. *Mathematical Models and Methods in Applied Sciences*, 28(05):953–978, 2018.
[20] Miroslav Kuchta. Assembly of multiscale linear PDE operators. In *Numerical Mathematics and Advanced Applications ENUMATH 2019: European Conference, Egmond aan Zee, The Netherlands, September 30-October 4*, pages 641–650. Springer, 2020.
[21] Miroslav Kuchta, Federica Laurino, Kent-Andre Mardal, and Paolo Zunino. Analysis and approximation of mixed-dimensional PDEs on 3D-1D domains coupled with Lagrange multipliers. *SIAM Journal on Numerical Analysis*, 59(1):558–582, 2021.
[22] Federica Laurino and Paolo Zunino. Derivation and analysis of coupled PDEs on manifolds with high dimensionality gap arising from topological model reduction. *ESAIM: Mathematical Modelling and Numerical Analysis*, 53(6):2047–2080, 2019.
[23] Anders Logg, Kent-Andre Mardal, and Garth Wells. *Automated solution of differential equations by the finite element method: The FEniCS book*, volume 84. Springer Science & Business Media, 2012.
[24] Luka Malenica, Hrvoje Gotovac, Grgo Kamber, Srdjan Simunovic, Srikanth Allu, and Vladimir Divic. Groundwater flow modeling in karst aquifers: Coupling 3D matrix and 1D conduit flow via control volume isogeometric analysis—experimental verification with a 3D physical model. *Water*, 10(12):1787, 2018.
[25] Rami Masri, Boqian Shen, and Beatrice Riviere. Discontinuous Galerkin approximations to elliptic and parabolic problems with a Dirac line source. *ESAIM: Mathematical Modelling and Numerical Analysis*, 57(2):585–620, 2023.
[26] Rami Masri, Marius Zeinhofer, Miroslav Kuchta, and Marie E Rognes. The modelling error in multidimensional time-dependent solute transport models. *arXiv preprint arXiv:2303.17999*, 2023.
[27] Luca Possenti, Giustina Casagrande, Simone Di Gregorio, Paolo Zunino, and Maria Laura Costantino. Numerical simulations of the microvascular fluid balance with a non-linear model of the lymphatic system. *Microvascular Research*, 122:101–110, 2019.
[28] Béatrice Rivière. *Discontinuous Galerkin methods for solving elliptic and parabolic equations: theory and implementation*. SIAM, 2008.
[29] Eduard Rohan, Vladimír Lukeš, and Alena Jonášová. Modeling of the contrast-enhanced perfusion test in liver based on the multi-compartment flow in porous media. *Journal of Mathematical Biology*, 77(2):421–454, 2018.
[30] L Ridgway Scott and Shangyou Zhang. Finite element interpolation of nonsmooth functions satisfying boundary conditions. *Mathematics of Computation*, 54(190):483–493, 1990.
[31] Rüdiger Verfürth. A review of a posteriori error estimation techniques for elasticity problems. *Computer Methods in Applied Mechanics and Engineering*, 176(1-4):419–440, 1999.
[32] Vegard Vinje, Erik NTP Bakker, and Marie E Rognes. Brain solute transport is more rapid in periarterial than perivenous spaces. *Scientific Reports*, 11(1):1–11, 2021.
[33] Haijun Wu and Yuanming Xiao. An unfitted hp-interface penalty finite element method for elliptic interface problems. *Journal of Computational Mathematics*, 37(3):316, 2019.